Trade-offs in Repetitive Control

Gunnar Hillerström Richard C.H. Lee

CUED/F-INFENG/TR 294

June 1997

Gunnar Hillerström
University of Cambridge
Department of Engineering
Trumpington Street
Cambridge CB2 1PZ
England
gh2@eng.cam.ac.uk

Richard C.H. Lee
University of Cambridge
Department of Engineering
Trumpington Street
Cambridge CB2 1PZ
England
rchl@eng.cam.ac.uk

Abstract. This report focuses on trade-offs between robustness and transient response for continuous time SISO LTI repetitive control systems. The transient is measured using various induced norms; whereas the robustness is quantified by the gap metric. In this evaluation the design tools used are $\mathcal{H}_\infty$ loop shaping and closed loop pole placement. For illustration, several first and second order plants are studied. In the appendix, Maple and Matlab codes are included.

1 Introduction

The aim of this report is to answer some fundamental questions about robustness and performance of continuous time SISO LTI repetitive control systems, with internal models to asymptotically reject periodic disturbances.[1]

As a performance measure we look at the transient due to e.g. a step, as it is commonly used for checking controller designs. Also, a power-energy induced norm measuring the worst case transient, given that the input signal comprises the modelled frequencies, is used.

Earlier work on sampled data repetitive control systems, shows that the delay margin is in general very poor [14, 4, 5]. Here the alternative gap metric robustness margin [3] is used as robustness measure. This has been used earlier in the context of repetitive control in [10, 11].

The primary focus is on disturbance rejection, where the disturbance is injected at the plant input. In this case the one-degree of freedom (Fig. 1) controller C interconnected with plant P, is sufficient. Of course, the plant can only be modelled up to a certain accuracy, and here coprime factor plant uncertainty [3, 18] is considered in the control design. The trade-offs between the transient performance and the robustness will be discussed.

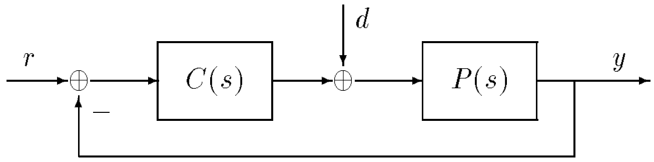

Figure 1: One-degree of freedom controller.

1.1 Design Tools

Two design methods are used throughout this report, namely, robust control design using $\mathcal{H}_\infty$ loop shaping and placement of the closed loop poles. It is assumed that the plant $P(s) \doteq B(s)/A(s)$, as a coprime fraction, is real-rational and strictly proper whereas the controller $C(s) \doteq S(s)/R(s)$, as a coprime fraction, is real-rational and proper. Without loss of generality, $A(s)$ and $R(s)$ are assumed to be monic. The internal model is denoted by H, e.g. for integral control $H(s) = s$; for a single sinusoid of angular frequency ω_0, $H(s) = s^2 + \omega_0^2$.

[1] In repetitive control both rejection of periodic disturbances, and tracking of periodic references are treated simultaneously. Here we focus on the harder (in the sense that you do not have access to the disturbance signal, in contrast to the reference signal) of the two problems.

1.1.1 Loop Shaping

For details and definitions about the gap metric robustness margin and the $\mathcal{H}_\infty$ loop shaping method, the reader is referred to [13, 3, 18] and Section 3. For simplicity, here, we just mention the procedure of the loop shaping method:

1. Loop shaping: Use a weighting function $W(s)$ such that the weighted nominal plant has a desired open loop shape.
2. Robust stabilization:
   a) Calculate the optimal robustness margin for the weighted plant. If the optimal robustness margin is too small, return to Step (1) and adjust the weight $W(s)$.
   b) Synthesize the optimal controller $C_{\text{opt}}(s)$.
3. The final feedback controller $C(s)$ is then constructed by combining the controller $C_{\text{opt}}(s)$ with the weighting function $W(s)$, i.e. $C_W(s) \doteq W(s)C_{\text{opt}}(s)$.

The weighting function $W(s)$ throughout this report is simply selected to be

$$W_\beta(s) \doteq \frac{H(s+\beta)}{H(s)} \quad , \quad \beta > 0. \tag{1}$$

For example if we include d.c. (integral action) and a pure sinusoid of frequency ω_0 we may take

$$W_\beta(s) = \frac{(s+\beta)\left((s+\beta)^2+\omega_0^2\right)}{s(s^2+\omega_0^2)}. \tag{2}$$

For β small, the poles and zeros of $W_\beta(s)$ will be close together; and as will be shown in the sequel, this gives a controller $C_{W_\beta}(s)$ with $b_{P,C_{W_\beta}}$ close to the optimal value, at the expense of a bad transient performance [10, 11]. A larger value of β will give better performance, but worse robustness. So, the selection of β clearly reflect the trade-off between transient performance and robustness.

When the controller $C_{W_\beta}(s) = W_\beta(s)C_{\text{opt}}(s)$ is formed, the zeros of $H(s)$ will be poles of the controller, as prescribed by the Internal Model Principle [2]. This gives an infinite open loop gain for the modelled frequencies, and thereby zero steady state error for these frequencies, provided the closed loop is stabilized.

Note that, even though stability in terms of the closed loop poles will be the same, the $b_{P,C}$ alters, if you put the weighting function $W(s)$ as being a part of the plant or being a part of the controller. The optimal controller

$C_{\rm opt}(s)$ is derived for the weighted plant $W(s)\,P(s)$, and thereafter $C_W(s)$ is implemented. Normally, if $b_{WP,C_{\rm opt}}$ is good for the weighted plant, it is not too bad for the plant being controlled by the controller $C_W(s)$.

From [18] we know that the optimal controller for the weighted plant will be of order $\deg\{A\} + \deg\{H\} - 1$, giving a final controller $C_W(s)$ of order $\deg\{A\} + 2\deg\{H\} - 1$. As will be seen in the pole placement design below, this controller may be of an unnecessarily high order. A simplified controller, for practical purposes, will be obtained by a model reduction step.

1.1.2 Pole Placement

The characteristic polynomial determining the closed loop poles is given by

$$A_m(s) \doteq A(s)R(s) + B(s)S(s) \doteq \prod_{i=1}^{m}(s+p_i). \tag{3}$$

As $\deg\{AR\} > \deg\{BS\}$ this A_m will be a polynomial equation of order $m \doteq \deg\{AR\}$.

The transfer function from the disturbance $\hat{d}(s)$ to the output $\hat{y}(s)$ (Fig. 1) is given by

$$G_d \doteq \frac{P}{1+CP} = \frac{BR}{A_m} \tag{4}$$

So, by including H as a factor of R, the modelled frequencies will be "blocked" from affecting the output. This is an alternative to the high gain interpretation of the Internal Model Principle, but leads to the same, H being in the denominator of the controller, or $R = H\,R'$.

In the framework of pole placement we obtain two things: 1) the minimal extra dynamics needed to stabilize the plant with the internal model, and 2) by e.g. placing all poles at the same point, $A_m = (s+p_1)^m$, we just as for loop shaping, get one parameter $p_1 > 0$ which may be utilized to depict possible trade-offs between robustness and the transient performance. This particular pole placement is also reasonable because it brings the system to zero error in the shortest possible time without overshoot. With all poles being equally fast, there are no unnecessary fast modes (requiring large control signals) [7]. As will be shown below in Section 4, this kind of "fastest" transient, does not necessarily minimize the 2-norm. In fact, it will be reduced by allowing an overshoot.

The minimal order controller with the internal model, will have the same amount of extra dynamics as without it. This is due to the fact that, including the model H in the denominator of the controller, we get the freedom to select just as many zeros while still preserving causality of the controller.

To show this, we use the simplest case of the algorithm included in the appendix of [15], which gives the total number of poles in the system (plant plus controller)

$$m = 2\,\deg\{A\} + \deg\{H\} - 1 \tag{5}$$

and to be able to solve the design equation (3)

$$\deg\{R'\} = m - \deg\{A\} - \deg\{H\} = \deg\{A\} - 1 \tag{6}$$

just as *without* the internal model. The polynomial S, the numerator of the controller, will include the extra parameters needed to obtain free pole placement

$$\deg\{S\} = \deg\{A\} + \deg\{H\} - 1. \tag{7}$$

An important question, which is sometimes used as an argument *against* the use of repetitive control, is that the controller will be of high order. Including the model H inevitably gives this extra dynamics, but in general no more; at least not to obtain full pole placement. The problem is that, with this lowest order controller, we might not meet the specifications in terms of robustness and transient performance simultaneously. It is, of course, possible to include extra dynamics in the controller, and guidelines for doing this may be found in [15]. Alternatively, we may use loop shaping with a controller order reduction step. It is merely a matter of taste which of the tools being selected for design. The $b_{P,C}$ and energy of the transient though, gives quantitative measures of how well a particular design will perform. Trade-offs and limitations will become clearer from the simulations in Section 4.

2 Transient Performance

By including the internal model in the closed loop and stabilizing it, asymptotic rejection of the modelled harmonics is obtained [12, 8, 16, 6]. In addition it is, of course, desirable to have a fast transient, to quickly reach the state of perfect rejection of the modelled signals.

The class of disturbances $\mathcal{D}_n$ being considered here is

$$d(t) = 1_+(t) \sum_{\omega_k \in \Omega_n} a_k\, e^{j\omega_k t}$$

where $\Omega_n \doteq \{\omega_1, \ldots, \omega_n\}$, $a_k \in \mathbb{C}$, and

$$1_+(t) \doteq \begin{cases} 1, & t \geq 0 \\ 0, & t < 0 \end{cases} .$$

This allows the possibility of taking an arbitrarily large number of harmonics from a periodic signal or to consider some almost periodic disturbances.

Consider a signal $d(t) \in \mathcal{D}_n$ which is input to a stable SISO system $G_d(s)$ given by (4). The output $\hat{y}(s)$ can be decomposed into steady state $\hat{y}_{\rm ss}(s)$ and finite energy transient state $\hat{y}_{\rm tr}(s)$: $\hat{y}(s) = \hat{y}_{\rm ss}(s) + \hat{y}_{\rm tr}(s)$ where

$$\hat{y}_{\rm ss}(s) = \sum_{\omega_k \in \Omega_n} \frac{G_d(j\omega_k)}{s - j\omega_k} a_k$$

and

$$\hat{y}_{\rm tr}(s) = \sum_{\omega_k \in \Omega_n} \frac{G_d(s) - G_d(j\omega_k)}{s - j\omega_k} a_k.$$

(The transient state $\hat{y}_{\rm tr}$ has finite energy even for $\Omega_\infty = \{k\omega_0 : k \in \mathbb{Z}\}$ [9].)

Now suppose that $G_d(s) = C(sI - A)^{-1}B$ where A is stable. Let L_0 be the observability grammian matrix with respect to this state-space realization, i.e.

$$L_0 = \int_0^\infty e^{tA^*} C^* C e^{tA}\ dt \geq 0$$

and $A^* L_0 + L_0 A + C^* C = 0$. Then

$$\frac{G_d(s) - G_d(j\omega_k)}{s - j\omega_k} = -C(sI - A)^{-1}(j\omega_k I - A)^{-1} B$$

for each k and the time domain transient is

$$y_{\rm tr}(t) = -1_+(t)\, C e^{tA} \sum_{\omega_k \in \Omega_n} (j\omega_k I - A)^{-1} B a_k.$$

Define the vector

$$\underline{a} := \begin{pmatrix} a_1 \\ \vdots \\ a_n \end{pmatrix}$$

and the $n \times n$ hermitian non-negative definite matrix

$$\mathcal{M} := \left(B^*(-j\omega_k I - A^*)^{-1} L_0 (j\omega_l I - A)^{-1} B \right)_{1 \leq k,l \leq n}.$$

We now consider the square of transient energy:

$$\begin{aligned} \|y_{\rm tr}(t)\|_2^2 &= \sum_{k=1}^n \sum_{l=1}^n a_k^* B^*(-j\omega_k I - A^*)^{-1} L_0 (j\omega_l I - A)^{-1} B a_l \\ &= \underline{a}^* \mathcal{M} \underline{a}. \end{aligned}$$

Note that

$$\|\underline{a}\|_2 = pow(d(t)) := \left(\lim_{T\to\infty} \frac{1}{T} \int_0^T |d(t)|^2\ dt \right)^{\frac{1}{2}}.$$

If we define $\|G_d\|_{\mathrm{tr}\leftarrow\mathcal{D}_n}$ to be the maximal transient energy $\|y_{\mathrm{tr}}(t)\|_2$ for signals $d(t)\in\mathcal{D}_n$ with $pow(d(t))\le 1$, then

$$\|G_d\|_{\mathrm{tr}\leftarrow\mathcal{D}_n} = \sqrt{\overline{\lambda}(\mathcal{M})}.$$

The objective of keeping this quantity small, is to minimize the initial transient. Also, a change in the disturbance signal shape (not frequency) will have a small effect on the output.

We now define the transient induced norms due to individual frequency and due to pure sine wave and pure cosine wave as:

$$\|G_d\|_{\omega_k} \doteq \left(\int_0^\infty \left|C\, e^{tA}(j\omega_k I - A)^{-1}B\right|^2\, dt\right)^{1/2} = \left\|\frac{G_d(s)-G_d(j\omega_k)}{s-j\,\omega_k}\right\|_2,$$

$$\|G_d\|_{\sin(\omega_k t)} \doteq \left\|\frac{\omega_k(G_d(s)-G_d(j\omega_k))}{s^2+\omega_k^2}\right\|_2,$$

and

$$\|G_d\|_{\cos(\omega_k t)} \doteq \left\|\frac{s(G_d(s)-G_d(j\omega_k))}{s^2+\omega_k^2}\right\|_2.$$

In the case $\omega_k = 0$, we denote the induced norm as $\|G_d\|_{\mathrm{step}}$.

The norms $\|G_d\|_{\omega_k}$, $\|G_d\|_{\sin(\omega_k t)}$, $\|G_d\|_{\cos(\omega_k t)}$ can be computed using residue calculus. We also obtain certain bounds:

$$\max_{\omega_k\in\Omega_n} \|G_d\|_{\omega_k} \le \|G_d\|_{\mathrm{tr}\leftarrow\mathcal{D}_n} \le \sqrt{\sum_{\omega_k\in\Omega_n} \|G_d\|_{\omega_k}^2},$$

$$\max\left\{\|G_d\|_{\sin(\omega_k t)}, \|G_d\|_{\cos(\omega_k t)}\right\} \le \frac{1}{2}\left(\|G_d\|_{\omega_k} + \|G_d\|_{-\omega_k}\right),$$

and

$$\|G_d\|_{\omega_k} \le \|G_d\|_{\sin(\omega_k t)} + \|G_d\|_{\cos(\omega_k t)}.$$

The power-energy induced norm $\|G_d\|_{\mathrm{tr}\leftarrow\mathcal{D}_n}$ will be used together with the 2-norm of the step response (being a standard measure of the magnitude of the transient) in the evaluation of different designs in the Section 4. Note that for $\Omega_1 = \{0\}$, then $\|G_d\|_{\mathrm{tr}\leftarrow\mathcal{D}_1} = \|G_d\|_{\mathrm{step}}$ is the energy shown at the output due to a step disturbance $d(t) = 1_+(t)$.

The following simple example shows the values of each transient induced norm due to individual frequency and the power-energy induced norm $\|G_d\|_{\mathrm{tr}\leftarrow\mathcal{D}_n}$. Take $\Omega_3 = \{\omega_1 = 0, \omega_2 = 1, \omega_3 = -1\}$ and the stable plant

$$P(s) = \frac{\sqrt{2}}{s+1}.$$

The controller was chosen to be

$$C(s;\gamma) = \frac{(s+1)\left((2\gamma+1)s^2+(\gamma^2+2\gamma)s+(\gamma^2+1)\right)}{\sqrt{2}s(s^2+1)},$$

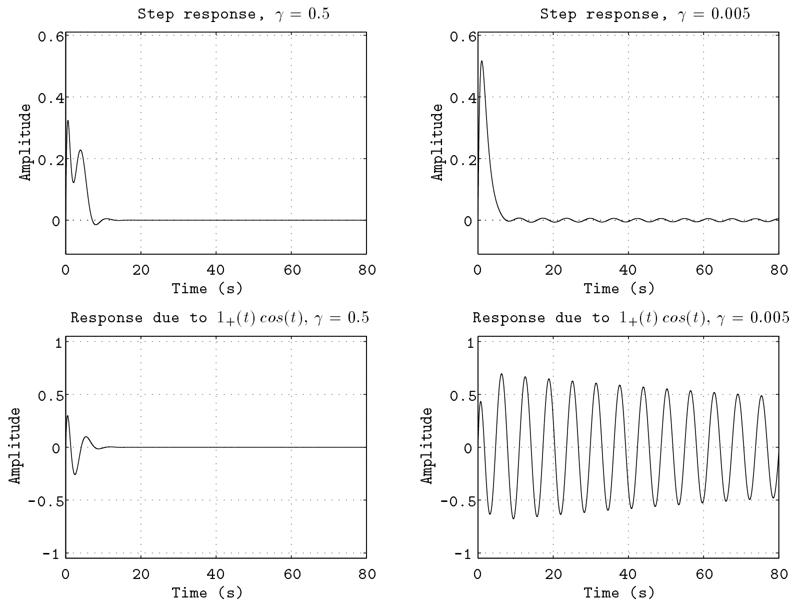

Figure 2: The time responses due to step disturbance and cosine disturbance for the systems $G_d(s;\gamma)$ with $\gamma = 0.5, 0.005$.

giving the closed loop

$$G_d(s;\gamma) = \frac{\sqrt{2}s(s^2+1)}{(s+1)^2((s+\gamma)^2+1)}.$$

Then the zeros of $G_d(s;\gamma)$ are exactly Ω_3 and the poles are $-1,-1,-\gamma \pm j$. This plant $G_d(s;\gamma)$ asymptotically rejects the frequencies in Ω_3. The time responses due to d.c. and $\cos(t)$ are shown in Figure 2. From the residue calculus, the closed form expressions for the transient induced norms

$$\|G_d(s;\gamma)\|_{\text{step}} = \sqrt{\frac{\gamma^3+4\gamma+4}{2(\gamma^6+4\gamma^5+9\gamma^4+12\gamma^3+12\gamma^2+8\gamma+4)}}$$

and

$$\|G_d(s;\gamma)\|_{\omega_2} = \|G_d(s;\gamma)\|_{\omega_3} = \frac{1}{\sqrt{2\gamma(\gamma^2+2\gamma+2)}}$$

can easily be computed. When considering the transient responses due to real sinusoids $\cos(t)$ and $\sin(t)$, the induced norms are:

$$\|G_d(s;\gamma)\|_{\sin(t)} = \sqrt{\frac{\gamma+1}{2\gamma(\gamma^4+4\gamma^3+8\gamma^2+8\gamma+4)}}$$

and

$$\|G_d(s;\gamma)\|_{\cos(t)} = \sqrt{\frac{\gamma^2+\gamma+1}{2\gamma(\gamma^4+4\gamma^3+8\gamma^2+8\gamma+4)}}.$$

γ	$\|G_d(s;\gamma)\|_{\text{step}}$	$\|G_d(s;\gamma)\|_{\omega_2}$, $\|G_d(s;\gamma)\|_{\omega_3}$	$\|G_d(s;\gamma)\|_{\text{tr}\leftarrow\mathcal{D}_n}$
0.5	0.4816	0.5547	0.5844
0.005	0.7053	7.0534	7.0535

γ	$\|G_d(s;\gamma)\|_{\sin(t)}$	$\|G_d(s;\gamma)\|_{\cos(t)}$	$\sqrt{\sum_{\omega_k\in\Omega_3}\|G_d(s;\gamma)\|^2_{\omega_k}}$
0.5	0.3768	0.4070	0.9205
0.005	4.9875	4.9875	9.9999

Table 1: Different values of transient induced norms for the systems $G_d(s;\gamma)$ for $\gamma = 0.5, 0.005$.

The corresponding values for $\gamma = 0.5, 0.005$ are shown in Table 1. Figure 3

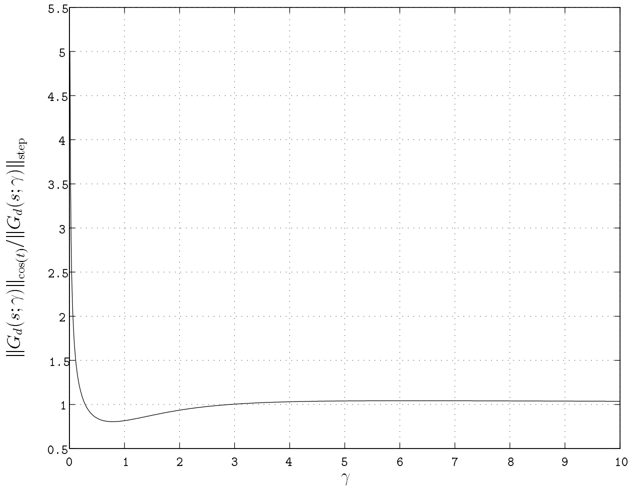

Figure 3: The ratio of the induced norms $\|G_d(s;\gamma)\|_{\cos(t)}$ and $\|G_d(s;\gamma)\|_{\text{step}}$ as a function of γ.

shows the ratio between the induced norms $\|G_d(s;\gamma)\|_{\cos(t)}$ and $\|G_d(s;\gamma)\|_{\text{step}}$ as a function of the parameter γ. As γ tends to zero, the closed loop system will have slow complex poles close to the imaginary axis and therefore the induced norm due to a cosine wave is much bigger than the induced norm due to a step; though both signals have a unit jump at $t = 0$. In this case, the controller action in rejecting $\cos(t)$ is very weak because the controller has zeros

$$\frac{-\gamma(\gamma+2) \pm j\sqrt{4+8\gamma+4\gamma^3-\gamma^4}}{2(2\gamma+1)}$$

close to its poles $\pm j$. For small γ, the controller is more robust towards plant uncertainties, though the transient performance is very poor. This robustness/transient performance trade-off will be seen in the later sections.

3 Robustness Towards Plant Uncertainty

The classical ways of measuring how *robust* a control system is, by phase, and gain margin. Using only one of them as robustness measure is however *not* enough because, even if one of them is good, the other one may be arbitrarily poor. *Here we use the gap metric [3] as a robustness measure:*

$$b_{P,C} \doteq \left\| \begin{pmatrix} I \\ P \end{pmatrix} (I + C\,P)^{-1}\,(I, C) \right\|_\infty^{-1}. \tag{8}$$

A good $b_{P,C}$ also implies both good phase, and gain margin (Theorem V.6, [17]):

$$GM(P,C) \geq \frac{1 + b_{P,C}}{1 - b_{P,C}},$$

and

$$PM(P,C) \geq 2 \arcsin(b_{P,C}).$$

A control system is normally considered as "sufficiently robust" if $b_{P,C} > 0.25$. In this case, a phase margin of 28.9° and a gain margin of 5/3 are guaranteed.

For SISO polynomial systems with $P \doteq B/A$ and $C \doteq S/R$, and characteristic polynomial $A_m = AR + BS$, (8) may be rewritten as [17]

$$b_{P,C}^{-1} = \sqrt{\sup_{s=j\omega} X(s)} \tag{9}$$

where

$$X(s) \doteq \frac{(A^*A + B^*B)\,(S^*S + R^*R)}{A_m^* A_m} \tag{10}$$

and e.g. $A^*(s) \doteq \overline{A(-\bar{s})}$ and similar for B, S, R and A_m. Consider $A = \prod(s + a_i), a_i \in \mathbb{C}$, then $A^*A = \prod(-s + a_i)(s + a_i) = \lambda + a_i^2$ with $\lambda \doteq -(j\,\omega)^2 = \omega^2$. So, taking the maximum over $\omega \in [-\infty, \infty]$ is replaced by $\lambda \in [0, \infty]$. Both S/R and B/A are proper, so X is biproper.

To write down X by hand, even for higher degree SISO systems is fairly easy; to get analytical expressions for the maximum is a much harder problem. If the λ candidates λ_c is sought by differentiation of[2]

$$X = \frac{\prod_{i=1}^m (\lambda + z_i)}{\prod_{i=1}^m (\lambda + p_i^2)},$$

[2]Note that z_i and p_i are non-transparent functions of the open loop controller and plant gains, poles and zeros.

then

$$\left.\frac{dX}{d\lambda}\right|_{\lambda=\lambda_c} = X(\lambda_c)\cdot\sum_{i=1}^{m}\left\{\frac{1}{\lambda_c+z_i}-\frac{1}{\lambda_c+p_i^2}\right\}=0.$$

As $X(\lambda_c)\neq 0$ for $\lambda_c \geq 0$,

$$\sum_{i=1}^{m}\frac{1}{\lambda_c+z_i}=\sum_{i=1}^{m}\frac{1}{\lambda_c+p_i^2}. \tag{11}$$

Again, $m=\deg\{A_m\}$. When rewriting this on a common denominator, you get an equation of order $2m-1$, and as we have a "1" as numerator on each fraction (the polynomials are monic), the highest order term vanishes, and thus a $2(m-1)$ order polynomial equation in λ_c.

For a first order A_m, $2(m-1)=0$, and therefore the only candidates are the end-points, namely $\lambda=0$ or $\lambda\to\infty$. For a second order A_m, $m=2$ and $2(m-1)=2$ we get (in addition to the points 0 and ∞) two possible candidates λ_c.

If we want to optimize analytically and freely over the possible closed-loop locations we are restricted to at most third order A_m (giving a polynomial equation of order 4); i.e. a first order plant with one modelled sinusoid is on the border of what may be analytically studied. If, however, we impose a restriction by placing k of the closed-loop poles at the same location we reduce the equation order by to $2(m-1)+1-k$. With all poles placed at the location, $k=m$, it may be reduced to degree $m-1$. For systems, controller plus plant poles, of order higher than four, no general analytical solution can be given. Even for lower order systems the expressions may be quite messy. Therefore, in most of the examples below, the calculations of both $b_{P,C}$ and the induced norms measuring the transient are performed numerically using Matlab.

Robustness limitation when including internal models With $H(s)=\prod_k(s^2+\omega_k^2)$ included in the controller, we may directly calculate a limit for the obtainable $b_{P,C}$ by noting that $H(\lambda)=-\lambda+\omega_k^2$, or $H(\lambda=\omega_k^2)=0$. Again noting that $R=R'H$, (10) gives

$$X(\lambda=\omega_k^2)\doteq\left.\frac{(A^*A+B^*B)\,S^*S}{(BS)^*(BS)}\right|_{\lambda=\omega_k^2}=\frac{1+|P(j\omega_k)|^2}{|P(j\omega_k)|^2} \tag{12}$$

There are possibly other λ's for which X takes its maximum, but at least (9),(12) gives the limitation of

$$b_{P,C}\leq\frac{|P(j\omega_k)|}{\sqrt{1+|P(j\omega_k)|^2}} \tag{13}$$

In fact, we know from [10, 11] that

$$b_{P,C} \leq b_{\mathrm{opt}}(P,\Omega_n) = \min_{\omega_k \in \Omega_n} \left(b_{\mathrm{opt}}(P), \frac{|P(j\omega_k)|}{\sqrt{1+|P(j\omega_k)|^2}} \right) \tag{14}$$

where the quantities $b_{\mathrm{opt}}(P)$ [3] and $b_{\mathrm{opt}}(P,\Omega_n)$ [10] are defined to be

$$b_{\mathrm{opt}}(P) \doteq \sup_{C \text{ stablz}} \{b_{P,C}\},$$

and

$$b_{\mathrm{opt}}(P,\Omega_n) \doteq \sup_{C \text{ stablz}} \{b_{P,C} : P(I+CP)^{-1}(j\omega_k) = 0 \;\; \forall \omega_k \in \Omega_n\}.$$

If $|P(j\omega_k)|$ is small for some ω_k we try to perfectly reject, the robustness margin will be poor. Or, conversely if we require a $b_{P,C} > \alpha$, say $\alpha = 0.25$, $|P(j\omega_k)| \geq (\alpha^{-2}-1)^{-1/2} \approx 0.58$ for all modelled frequencies ω_k.

The observant reader may of course argue against this result by reasoning that it is just a matter of increasing the output amplification by a factor of say k. As this robustness measure, unlike measures related to the open loop frequency response (Nyquist plots) e.g. phase and gain margin, will change if the plant $k\,P$ with controller C/k in the feedback loop is considered. In this case (13) will give

$$b_{kP,C/k} \leq b_{\mathrm{opt}}(kP,\Omega_n) \leq \frac{k\,|P(j\omega_k)|}{\sqrt{1+(k\,|P(j\omega_k)|)^2}}$$

So, by simply selecting a large enough k, the robustness limitation is eliminated. This is true in the sense that if we have not done the scaling properly beforehand, we now get a reminder to do so. Otherwise, if the signal range is already used fully, this is not an option.

4 Case Studies

In this section a number of first and second order system examples are studied. This enables to calculate the solutions analytically. The approach taken is to study robustness and transient performance in face of the pole placement design, as an application of the theory outlined in Section 2 and 3.

It is hard to analytically study higher order systems, especially with the $b_{P,C}$ based on the $\mathcal{H}_\infty$ norm. On the other hand, the norms measuring transient performance are easier to calculate, e.g amounting to a sum of residues. As the system grows larger, the expressions gets messier; but in principle the calculation is straight-forward. For the $b_{P,C}$ in SISO systems, it amounts to calculate the maximum of a biproper real-rational function.

So, numerically it is a simple search, but analytical solutions are very hard to derive. We therefore introduce numerical solutions, such as the `emargin` function in Matlab, where analytical solutions are too hard, or too time consuming, to get. The Maple and Matlab codes for the computations of the transient induced norms and robustness margins, may be found in the Appendix of this report.

4.1 Basics, Without Internal Model

With the plant as

$$P(s) = \frac{B(s)}{A(s)} = \frac{k}{s\tau + 1}$$

the optimally robust controller will be of order $\deg\{A\}-1 = 0$, say $C(s) = c$.

Robustness For this simple case, the largest value of X must be at the endpoints $\lambda = 0$ or ∞; and therefore it is fairly straightforward to calculate the robustness margins for the general first order system.

$$X(\lambda; c) = \frac{\left(\lambda\,\tau^2 + 1 + k^2\right)\left(c^2 + 1\right)}{\lambda\,\tau^2 + (1 + ck)^2}$$

which has its maximum at $\lambda = 0$ for "small" c (or $c \leq c_\star$, defined below) with

$$X(\lambda = 0; c) = \frac{(1 + k^2)(1 + c^2)}{(1 + c\,k)^2}$$

and at $\lambda \to \infty$, for $c > c_\star$ with

$$\lim_{\lambda\to\infty} X(\lambda; c) = 1 + c^2.$$

The optimal $c_\star = \frac{-1+\sqrt{1+k^2}}{k} \in (\,0, 1\,)$, is such that $(1 + k^2) = (1 + c\,k)^2$, and therefore

$$\sup_{\lambda\geq 0} X(\lambda; c_\star) = \frac{2\,(1 + k^2 - \sqrt{1 + k^2})}{k^2}.$$

Substituting into (9) gives

$$b_{\mathrm{opt}}(P) = b_{P,c\star} = \frac{k}{\sqrt{2\,(1 + k^2 - \sqrt{1 + k^2})}} \in \left(\frac{1}{\sqrt{2}}, 1\right).$$

For this plant an analytical expression for $c > c_\star$ such that

$$b_{P,C} = \frac{1}{\sqrt{1 + c_\alpha^2}} = \alpha$$

is $c_\alpha = \sqrt{\alpha^{-2} - 1}$.

Noting that c_α is independent of both the plant parameters k and τ, we remark that this is more of an exercise to illustrate the calculations. We have, in this case, taken the robustness measure to far from classical control theory. In this case we should have used a frequency weighted $b_{P,C}$ [3, 13, 1]. We may, however, conclude that the optimal robustness margins for first order systems is, as expected, very good.

Transient Performance Here there is no internal model included in the design, nevertheless we calculate the 2-norm of the transfer function $G_d(s)$

$$\begin{aligned}
\|G_d(s;c)\|_2^2 &= \left\|\frac{P(s)}{1+P(s)C(s)}\right\|_2^2 = \left\|\frac{k}{s\tau+1+ck}\right\|_2^2 \\
&= \operatorname{Res}\left\{\frac{k^2}{(-s\tau+1+ck)(s\tau+1+ck)};\ s=p_1=-\frac{1+ck}{\tau}\right\} \\
&= \frac{k^2}{2\tau(1+ck)} \\
\Rightarrow \|G_d(s;c)\|_2 &= \frac{k}{\sqrt{2\tau(1+ck)}}
\end{aligned}$$

which in effect is the energy of the signal shown at the output due to an impulse disturbance ($\hat{d}(s)=1$).

With relaxed robustness, the transient performance is better.

$$\frac{\|G_d(s;c_\alpha)\|_2}{\|G_d(s;c_\star)\|_2} = \sqrt{\frac{1+c_\star k}{1+c_\alpha k}}\ \left(=\sqrt{\frac{\sqrt{1+k^2}}{1+k\sqrt{\alpha^{-2}-1}}}\right) \leq 1.$$

4.2 With I- and PI-control

As a simple case of the internal model, we first study a first order plant with Integral (I) or Proportional Integral (PI) control. For the purpose of illustration, the plant in this section is selected to be

$$P(s) = \frac{10}{s+1}$$

with time constant $\tau = 1$ s and static gain $k = 10$. From the above analysis of first order systems, we know that the optimal robustness is very good, $b_{\text{opt}}(P) \approx 0.74$.

4.2.1 First Order Plant With a Pure I-control

I-control for a first order system, is somewhat restricted, in the sense that it slows down the closed loop. Disregarding this, it will give us simple analytical solutions for both robustness and transient performance.

Analysing this problem from a root locus perspective, the root-locus will start out in the open loop poles at $s = 0$ and $s = -1$, approaching $s = -1/2$ and then shooting off $90°$ onto the complex plane. The closed loop poles will thus be be located either as $s = -1/2 \pm b_r$ on the real axis or as $s = -1/2 \pm j\, b_j$. The controller will in those cases be given by

$$C(s) = \frac{(1 - 4\, b_r^2)}{40\, s} \quad ; \ |b_r| < 1/2$$

and

$$C(s) = \frac{(1 + 4\, b_j^2)}{40\, s}$$

respectively.

Transient Performance Notice that with A_m stable, and the model $H(s) = s$ included as $R = R'H$, the transfer function $BR/(sA_m) = BR'/A_m$ is strictly proper and has no poles on the imaginary axis. Therefore its 2-norm is finite, and given by

$$\|BR'/A_m\|_{\text{step}}^2 = \sum_{i=1}^{n} \text{Res}\left\{\frac{B^* R'^*\, BR'}{A_m^*\, A_m};\ p_i\right\} \tag{15}$$

where p_i is the closed loop poles as before.

With $B\,R'/A_m = 10/((s + 1/2 + b_r)(s + 1/2 - b_r))$, (15) gives

$$\|BR'/A_m\|_{\text{step}}^2 = \frac{200}{1 - 4\, b_r^2} \quad ; \ |b_r| < 1/2$$

which is minimized by $b_r = 0$, which in turn gives the best performance. Thus, if we restrict the poles for the second order system to lie on the negative real axis, not surprisingly, the best performance is obtained with a double pole.

If we go off axis, introducing oscillatory closed loop poles, (15) gives

$$\|BR'/A_m\|_{\text{step}}^2 = \frac{200}{1 + 4\, b_j^2} \tag{16}$$

by selecting a large enough b_j, an arbitrary small transient may be obtained. The limitation, as will be shown in the sequel, will be robustness.

Robustness For the interesting part where the root-locus is branching out from the double pole in $s = -1/2$, (10) gives[3]

$$X(\lambda; b_j) = \frac{(\lambda + 101)\,(\lambda + ((1 + 4\, b_j^2)/40)^2)}{(\lambda + (1/2 + j\, b_j)^2)\,(\lambda + (1/2 - j\, b_j)^2)}$$

[3] Even if there are imaginary factors of X, they appear as complex conjugates. Therefore the overall function is still real (and strictly positive) for all $\lambda \geq 0$.

For the double pole corresponding to $b_j = 0$, and assuming $1/1600 \ll \lambda_c \ll 101$, (11) gives

$$\frac{1}{\lambda_c + 101} + \frac{1}{\lambda_c + 1/1600} \approx \frac{1}{\lambda_c} = \frac{2}{\lambda_c + 1/4}$$

or $\lambda_c \approx 0.25$ and finally the maximum $X(\lambda_c) \approx 101$, giving a fairly low robustness margin of $b_{P,C} \approx 0.10$. If the transient is reduced by selecting $b_j > 0$, (11) gives a second order equation in λ_c, still with only one positive root. Calculating $X(\lambda_c)$ shows that $b_{P,C}$ decreases monotonically from 0.10 down to 0.05 when b_j increases from 0 to 10. As the robustness is bad enough for $b_j = 0$, the details are omitted, but similar to the calculations performed with the PI-control below.

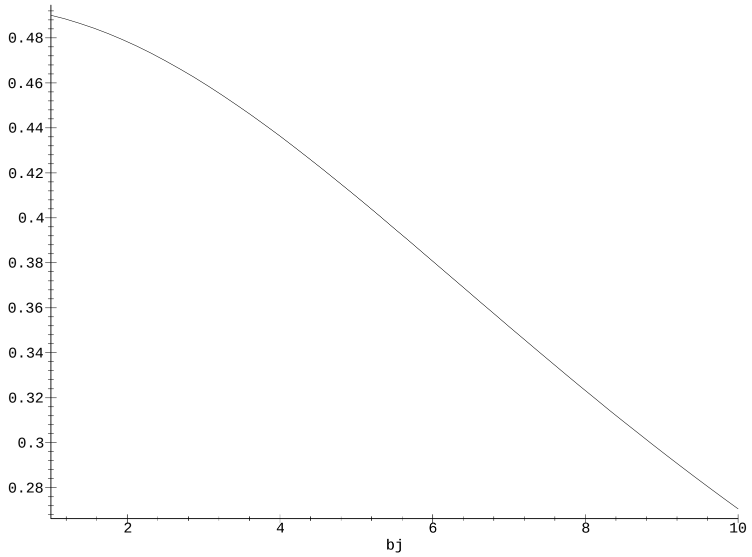

Figure 4: $b_{P,C}$ depicted as a function of $b_j \in [0, 10]$ using PI-control.

4.2.2 First Order Plant With PI-control

To get both better transient and robustness, PI control, placing the poles in $s = -3 \pm j\, b_j$, is used with the above first order plant. This enables to reduce the transient

$$||BR'/A_m||^2_{\text{step}} = \frac{25}{3\,(9 + b_j^2)} \tag{17}$$

by increasing b_j.

For this pole placement (10) gives

$$X(\lambda; b_j) = \frac{(\lambda + 101)\left(125\,\lambda + (9 + b_j)^2\right)}{100\,(\lambda + (3 + j\,b_j)^2)(\lambda + (3 - j\,b_j)^2)}.$$

Instead of giving the actual expressions of λ_c from (11) and the $b_{P,C}$ from (9), the calculations are performed using Maple, and then approximated by a polynomial of degree 3; giving an error of less then 0.003 for $b_j \in [0, 10]$

$$b_{P,C} \approx 0.4962 - 3.864 \cdot 10^{-4}\, b_j\,(1 + 12.1\, b_j - 0.64\, b_j^2). \tag{18}$$

A plot of the analytically calculated $b_{P,C}$ is also given in Fig. 4. So, as we move off axis from a reasonably fast pole placement, performance may be improved according to (17) at the expense of robustness (18).

To conclude this first order example, the closed loop poles are placed in $s = -a \pm j\,b$ using

$$C(s) = \frac{(2\,a - 1)\,s + a^2 + b^2}{10\,s}$$

for which the transient given by (15)

$$||BR'/A_m||^2_{\text{step}} = \frac{25}{a\,(a^2 + b^2)}. \tag{19}$$

So, the transient will be smallest for closed loop poles as far to the left in the s-plane as possible (large a and large $a^2 + b^2$).[4] For computing $b_{P,C}$ (10) gives

$$X(\lambda; a, b) = \frac{(\lambda + 101)(\lambda\,(101 + 4a\,(a - 1)) + (a^2 + b^2)^2)}{100\,(\lambda + (a + j\,b)^2)(\lambda + (a - j\,b)^2)}. \tag{20}$$

Solving (11), and checking the sign of the possible candidate λ_c, substituting into (20) and taking the maximum of $X(\lambda_c)$ and the endpoints ($\lambda = 0$, $\lambda \to \infty$) gives $b_{P,C}(a, b)$. This function seems hard to be approximated by a multivariate Taylor series expansion; and instead of giving the actual expression, a contour plot for $b_{P,C}(a, b) \geq \alpha$, $\alpha \in \{0.2, 0.3, 0.4, 0.5\}$ is given in Fig. 5. This graph is also validated using the corrected version of `emargin` in Matlab.

4.3 First Order Plant

As an illustration we here select, being the same plant as in Section 2,

$$P(s) = \frac{\sqrt{2}}{s + 1}$$

[4] Note that the 2-norm for the transient will not be affected by inserting the proportional component to the controller, i.e. (19) with $a = 1/2$ coincides with the expression given by (16).

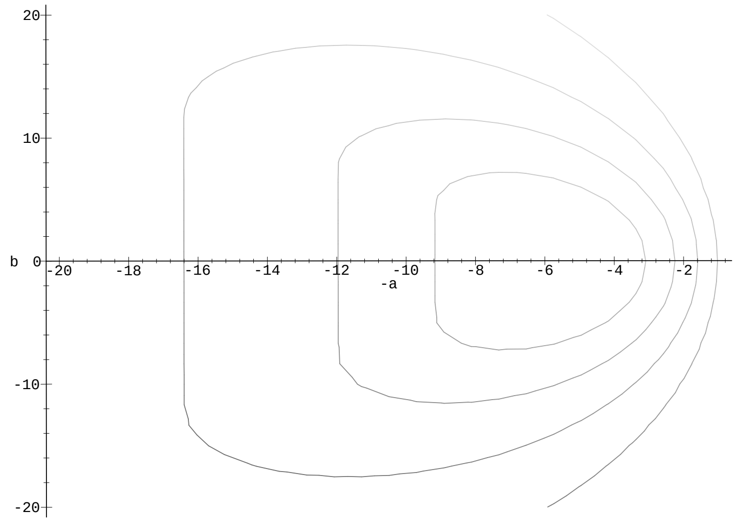

Figure 5: Robustness regions $b_{P,C} \geq \alpha$ for $\alpha \in [0.2, 0.3, 0.4, 0.5]$ using PI-control, depicted as a function of pole placement with $A_m = (s + a + j\,b)\,(s + a - j\,b)$.

with a crossover frequency of 1 rad/s and $b_{\mathrm{opt}}(P) \approx 0.89$. In the following subsection, the internal model comprises $\Omega_2 = \{\pm\omega_0\}$ with $H(s) = s^2 + \omega_0^2$; and thereafter extended to $\Omega_3 = \{0, \pm\omega_0\}$ with $H(s) = s\,(s^2 + \omega_0^2)$. The closed loop poles are chosen to have the same negative real parts.

4.3.1 With One Modelled Sinusoid $H(s) = s^2 + \omega_0^2$

The minimal number of poles in the system will be three ($m = 3$). To enable to illustrate $b_{P,C}$ as a function of the closed loop poles for different ω_0 in the plane, some kind of restriction on the degree of freedom for pole placement must be made. In this case the closed loop poles are selected to be equally fast, in the sense that they all have the same negative real part a, and thus

$$C(s) = \frac{(3\,a - 1)\,s^2 + (3\,a^2 + b^2 - \omega_0^2)\,s - \omega_0^2 + a(a^2 + b^2)}{\sqrt{2}(s^2 + \omega_0^2)} \tag{21}$$

giving $A_m = ((s + a)^2 + b^2)\,(s + a)$ is chosen.

Since no integral part is included, we cannot measure transient performance in terms of $\|G_d(s)\|_{\mathrm{step}}$ as it is not finite, instead we could use the transient due to $d(t) = \cos(\omega_0 t)\,1_+(t)$,

$$\|G_d(s)\|^2_{\cos(\omega_0 t)} = \frac{a}{2\,(4\,a^2 + b^2)}. \tag{22}$$

Note that with $d(t) = sin(\omega_0 t)\, 1_+(t)$, which does not have a jump in $t = 0$, a transient of

$$\|G_d(s)\|^2_{\sin(\omega_0 t)} = \frac{3\,\omega_0^2}{2\,a\,(4\,a^2 + b^2)\,(a^2 + b^2)}$$

being $3\,\omega_0^2/(a^2\,(a^2 + b^2))$ smaller, will arise. Returning to (22) we note again that, apart from the weighting, the expression for the 2-norm of the transient is similar to the latter one; thus the general guideline for minimizing the transient will the same as before: place the closed loop poles as far to the left as possible (on top of sufficient robustness).

For evaluation of robustness, the analytical expression for the controller given by (21) is used with the function `emargin` in Matlab to compute the $b_{P,C}$. Robustness as a function of pole placement is illustrated for different ω_0 in Fig. 6. For an internal model frequency of $\omega_0 = 0.1$, being well within the plant bandwidth, Fig. 6 shows that e.g. a triple pole on the negative real axis, around the location of the open loop plant pole, will give a good robustness. Allowing an overshoot by selecting two complex poles will, however, give a better transient performance in terms of the induced norms.

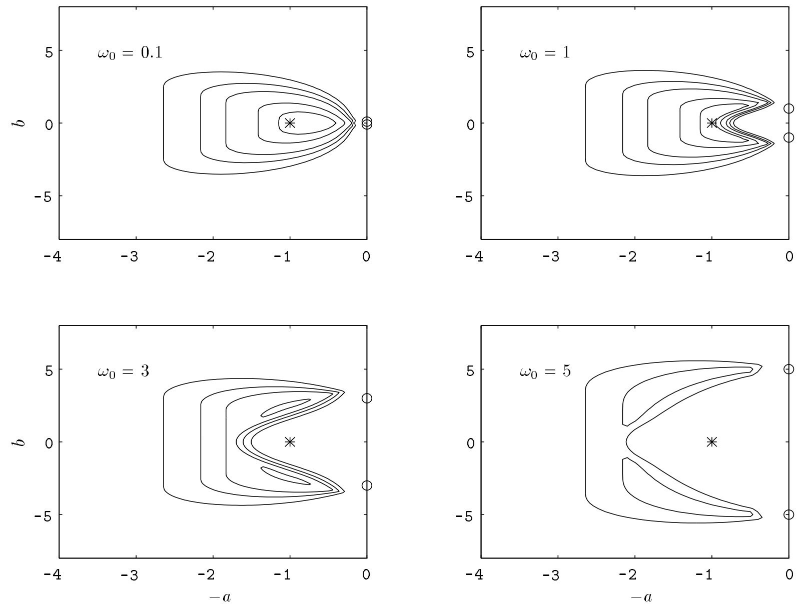

Figure 6: Robustness regions $b_{P,C} \geq \alpha$ for $\alpha \in [0.2, 0.25, 0.3, 0.4, 0.5]$ depicted as a function of pole placement with $A_m = (s + a + j\,b)\,(s + a - j\,b)\,(s + a)$ and $H(s) = s^2 + \omega_0^2$ for different ω_0; open loop plant and controller poles is marked by '$*$' and '$\circ$' respectively.

If the frequency ω_0 of the internal model is increased to $\omega_0 = 1$ rad/s, we get a horseshoe shape of the regions in Fig. 6. It is also clear where to place the closed loop poles to obtain a certain degree of robustness, and at the same time keep a good transient performance. General guidelines such as placing the poles "close" to both the modes of the plant and the controller, e.g. by selecting $A_m = ((s+1)^2+\omega_0^2)(s+1)$; even if it gives a robust controller, it may be improved upon both in terms of the transient performance and robustness by locating the closed loop poles further to the left and closer to the real axis.

If the frequency of the internal model mode is increased to $\omega_0 = 3$, $|P(j\cdot 3)| \approx 0.45$ which according to (14) gives $b_{P,C} \leq 0.408$. From Fig. 6 we get that $A_m = (s+1)((s+1)^2+\omega_0^2)$ will still give a robust controller. By reducing the complex part, the robustness will also in this case be improved. The transient performance may again be improved by moving the closed loop poles further to the left. For $\omega_0 = 5$, the limit for the $b_{P,C} \leq 0.267$ is given by (14). The controllers located within the smallest regions, with $b_{P,C} \geq 0.25$, are close to optimal robustness. Also here the transient performance given by (22) may be improved; but as shown in Fig. 6 e.g. placing all the poles on the negative real axis will not give a $b_{P,C} > 0.25$. The basic limitation here is the low plant gain at the modelled frequency [10, 11].

4.3.2 With I-control and One Modelled Sinusoid $H(s) = s(s^2+\omega_0^2)$

In this section, different solutions obtained by loop shaping and pole placement will be evaluated in terms of the transient performance and robustness. To evaluate the performance of both pole placement and loop shaping design, the norms $\|G_d\|_{\mathrm{tr}\leftarrow\mathcal{D}_3}$ and $\|G_d\|_{\mathrm{step}}$ measuring the transient (which we want to keep as small as possible) are depicted as functions of $b_{P,C}$ (which we want to keep reasonably large). In the end we will also connect these to the type of contour plots, $b_{P,C}$ as a function of the closed loop pole location, as was used in the last section.

The controller

$$C(s) = \frac{(4\,a-1)\,s^3 + 6\,a^2\,s^2 + (2\,a\,\omega_0^2 - \omega_0^2 + 4\,a^3)\,s + a^2(a^2+\omega_0^2)}{\sqrt{2}\,s\,(s^2+\omega_0^2)}$$

gives a novel pole placement of $A_m = (s+a)^4$ where a should be roughly 1 to get a robust controller. A higher a gives a faster system, but also a smaller robustness margin. The loop shaping design is parameterized by β, the zero location of the weighting function given by (2). For β close to zero, the poles and zeros of the weighting function $W_\beta(s)$ are close together, giving a $b_{P,C}$ close to the optimal $b_{\mathrm{opt}}(P,\Omega_3)$ at the expense of a bad transient performance [10, 11].

It is well worth noting that the loop shaping design gives a controller of higher order than the minimal order (for free pole placement) which is used for the pole placement design. We thus expect that both better transient performance and better robustness may be obtained owing to the larger degree of freedom.

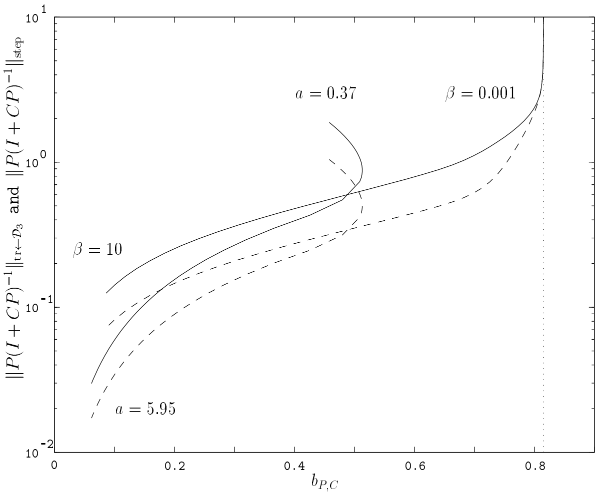

Figure 7: Loop shaping with $\beta \in [0.001, 10]$ and pole placement with $A_m = (s+a)^4$ and $a \in [0.37, 5.95]$; $H(s) = s^2 + 0.1^2$. $\|P(I+CP)^{-1}\|_{\mathrm{tr}\leftarrow\mathcal{D}_3}$: solid "—"; $\|P(I+CP)^{-1}\|_{\mathrm{step}}$: dashed "- -".

If a frequency well within the bandwidth of the open loop plant, $\omega_0 = 0.1$, is rejected, Fig. 7 shows that both pole placement and loop shaping give quite satisfactory designs, both in terms of robustness and transient performance. In this case the pole placement design will give better performance than the loop shaping using the weighting function W_β in (2), for the region of $b_{P,C} < 0.5$. In this region, the induced norms are offset approximately by a scaling factor, and therefore regardless of which of the norms being used for measuring the transient performance, the selected controller will be roughly the same.

Looking closer into the construction of the power-energy induced norm, shows that the signal which gives the worst case output is $d(t) \approx (1 + 2\cos\omega_0 t)/\sqrt{3}$, with $a_1 = a_2 = a_3 = 1/\sqrt{3}$. This signal, just as for $a_1 = a_2 = 0$, $a_3 = 1 \Rightarrow d(t) = 1_+(t)$, gives $\|\underline{a}\|_2 = 1$. In this case, because the closed loop poles are far from the imaginary axis, the difference between the step response and the response to $d(t) = (1 + 2\cos\omega_0 t)/3$, both having a unity jump at $t = 0$, is negligible[5] (Fig. 8). The transient, in this case, is largely determined by the jump in zero (as the signal is assumed to be zero for negative t) which equals $\sqrt{3}$ in the first case and 1 in the second. In this case the the induced norm corresponding to Ω_3 compared to Ω_1 may be up to 1.73 times larger, while the actual energy seen at the output is roughly the same. This is not a problem, as long as long as Ω_n is fixed; but one

[5]The ratio of the energy of the difference signal to the energy of the step response is less than 10^{-10}.

should bear this in mind when comparing different power-energy induced norms.

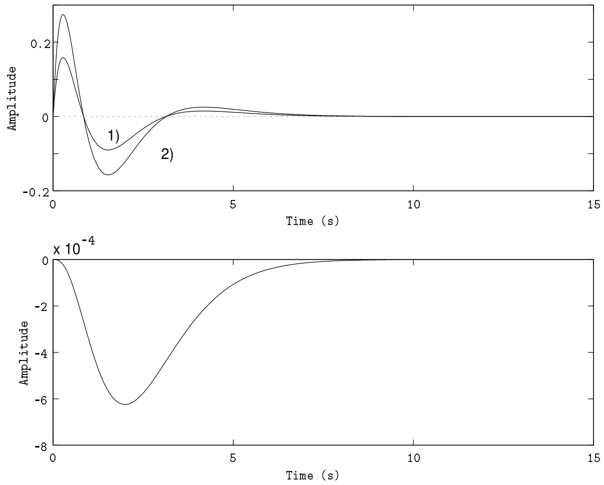

Figure 8: Top figure: closed loop response to 1) a step disturbance and 2) the disturbance $d(t) = (1 + 2\,\cos\omega_0\,t)/\sqrt{3}$ for pole placement design with $A_m = ((s + a)^2 + \omega_0^2)\,(s + a)^2$ and $a = 1.5$ giving $b_{P,C} \approx 0.27$, and the 2-norm of a 0.14 for the step response and the power-energy induced norm of 0.23 i.e. approximately 1.7 times larger. Bottom figure: difference between a step disturbance and the response to $d(t) = (1 + 2\,\cos\omega_0\,t)/3$, both having a unity jump at $t = 0$.

If we then try to reject $\omega_0 = 3$ rad/s, (14) gives that $b_{P,C} \leq 0.408$. Figure 9 shows that the loop shaping design still approach this limit for small β, while performance of the simple pole placement of $A_m = (s + a)^4$, is worse. If, instead, the more robust (closer to open loop poles) $A_m = ((s + a)^2 + \omega_0^2)\,(s + a)^2$ is selected, the both design methods give similar performance, Fig. 9.

Next we want to analyse the obtainable $b_{P,C}$ as a function of the pole placement, just as for the second and third order (plant plus controller order) systems above. As we here are faced with a fourth order system ($m = 3+1$), the graphs may be misleading, in the sense that better pole placement may be obtained utilizing the full freedom of pole placement. But, to be able to depict the plot in the plane two degrees of freedom must be fixed. In this case, this may be done by selecting

$$C(s) = \frac{(4\,a - 1)\,s^3 + (6\,a^2 + b^2 - \omega_0^2)\,s^2 + (2\,a\,b^2 - \omega_0^2 + 4\,a^3)\,s + a^4 + a^2\,b^2}{\sqrt{2}\,s\,(s^2 + \omega_0^2)}$$

giving $A_m = ((s + a)^2 + b^2)\,(s + a)^2$, which as before has the same negative real part but a double pole on the real axis and may be located close to the open loop poles in $s = 0$ and $s = -1$.

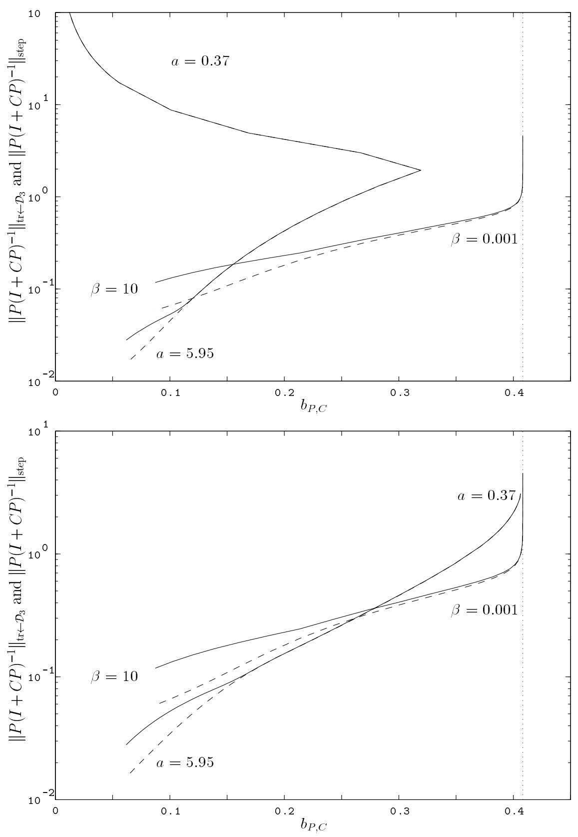

Figure 9: Loop shaping with $\beta \in [0.001, 10]$ and pole placement with for the top figure $A_m = (s+a)^4$ and for the bottom figure $A_m = ((s+a)^2 + \omega_0^2)(s+a)^2$ and $a \in [0.37, 5.95]$; $H(s) = s(s^2 + \omega_0^2)$ and $\omega_0 = 3$.

For an internal model frequency of $\omega_0 = 0.1$, being well within the bandwidth of the open loop plant, very good $b_{P,C}$ may be obtained. In fact, as seen from Fig. 10, selecting $A_m = (s + 0.6)^4$ will give a $b_{P,C} > 0.5$.

Note in Fig. 10 that when a increases (pole placement further to the left), the transient performance is improved, and therefore the transient induced norms are reduced. The curves for the induced norms as a function of the $b_{P,C}$ above, may therefore be seen as "slicing" the surfaces of Fig. 10 at $b = 0$ and $b = \omega_0$ parallel with the real axis. By doing this, we may explain the shapes of the curves in Fig. 7 and Fig. 9; and more importantly find better pole placements, approaching $b_{\text{opt}}(P, \Omega_n)$ or reducing the transient performance.

For $\omega_0 = 1$ rad/s, the shape again alters. It it clear from Fig. 10 that good $b_{P,C}$ may be obtained not only by locating the closed loop poles close to the open loop plant poles, but also close to the internal model modes included in the controller. With increased frequency ω_0 of the internal model, the

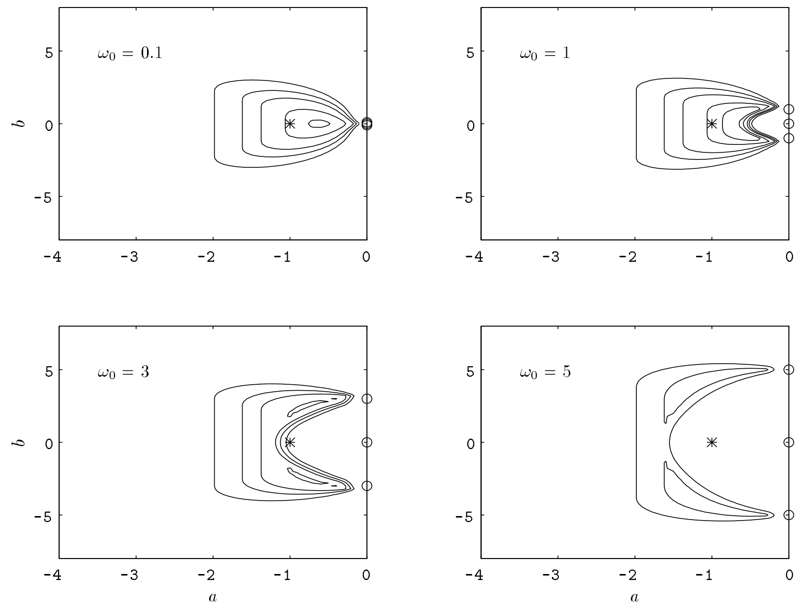

Figure 10: Robustness regions $b_{P,C} \geq \alpha$ with $\alpha \in \{0.2, 0.25, 0.3, 0.4, 0.5\}$ as a function of the pole placement, $A_m = ((s+a)^2 + b^2)\,(s+a)^2$ and $H(s) = s(s^2 + \omega_0^2)$ with different ω_0; open loop plant and controller poles is marked by '$*$' and '$\circ$' respectively.

maximum obtainable $b_{P,C}$ will be reduced according to (14). For $\omega_0 = 3$ rad/s, (14) gives $b_{P,C} \leq 0.408$; so the smallest islands in Fig. 10 again gives very close to optimal robustness, $b_{\text{opt}}(P, \Omega_3)$, the same is valid for $\omega_0 = 5$ where $b_{P,C} \leq 0.267$.

To conclude, for a first order system with integral control and one model sinusoid, it is fairly straightforward to place the closed loop poles to get the required robustness in terms of the $b_{P,C}$ and good transient performance. Comparing systems with the same $b_{P,C}$ with and without integral part of the controller, for the system with the integral part, the transient will be slower. For example, the maximum peaks for $b_{P,C}$ of Fig. 10 is closer to the origin than the ones of Fig. 6.

When we move up to higher order systems pole placement will be somewhat harder, mainly due to the fact that we only can have two degrees of freedom depicted in the plane. This may however to quite a large extent be overcome by using a combination of general guidelines, and fine-tuned by looking at graphs of obtainable $b_{P,C}$ in terms of the left free parameters; at the same time keeping in mind to minimize the transient, by selecting closed loop poles to the left in the regions.

4.3.3 Multiple Frequencies

The gain of the first order system decrease monotonically, so therefore the limit on $b_{P,C}$ given by (14) is determined by the highest frequency of the internal model, where the gain is lowest. By keeping $\max\{|\omega_k| : \omega_k \in \Omega_n\} = 3$ as in the last example, including lower harmonic frequencies of $\Omega_5 = \{0, \pm 1.5, \pm 3\}$, $\Omega_7 = \{0, \pm 1, \pm 2, \pm 3\}$ and $\Omega_9 = \{0, \pm 3/4, \pm 3/2, \pm 9/4, \pm 3\}$, (14) gives $b_{\text{opt}}(P, \Omega_k) \leq 0.408$ for $k \in \{3, 5, 7, 9\}$. From Fig. 11, which corresponds to Fig. 10 with $\omega_0 = 3$, but with more intermediate frequencies included, it is clear that the design becomes harder in the sense that $b_{P,C}$ decreases, using our closed loop pole placement. Also the peaks in Fig. 11 move towards the imaginary axis giving worse transient response.

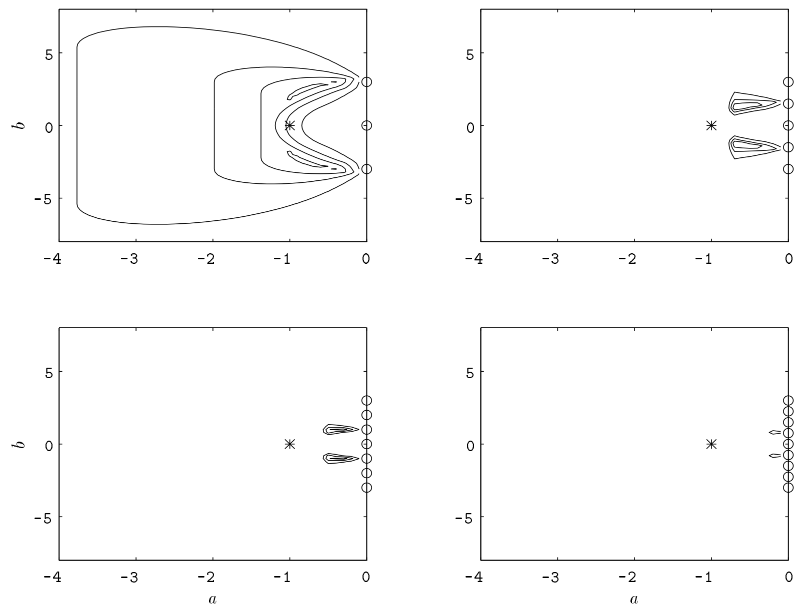

Figure 11: Robustness regions $b_{P,C} \geq \alpha$ with $\alpha \in \{0.1, 0.2, 0.3, 0.4, 0.5\}$ as a function of the pole placement, $A_m = (s+a)^2 \prod_{r=1}^{k}((s+a)^2 + (r\,b)^2)$, $k = \{1, 2, 3, 4\}$; with $\max(\omega_k) = 3$ rad/s; open loop plant and controller poles is marked by '$*$' and '$\circ$' respectively.

It may also be noted that, the way the pole placement is parameterized, the maximum robustness is by locating the first off axis pole close to the first internal modelled frequency pole. Again, this may not be the true picture, as it is restricted by the choice of poles to be able to depict $b_{P,C}$ in the plane. But it still gives an indication of that the design problem gets harder, despite no additional constraint is given by (14).

To get rid of the choice of poles, we next turn to loop shaping for the same internal model modes and plant. For comparing transient performance of different controllers, as the set of internal model frequencies Ω_n is varied,

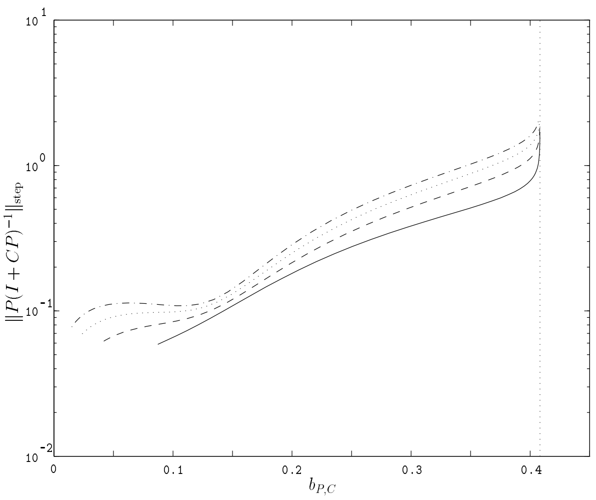

Figure 12: Loop shaping with $\beta \in [0.01, 10]$ and from below Ω_k, $k \in \{3, 5, 7, 9\}$ respectively.

referring to the discussion in Section 4.3.2, the 2-norm of the step response is used for the sake of comparison. From Fig. 12 two things are clear; 1) the design problem gets harder with more included frequencies, even though (14) does not impose further constraints, and 2) a $b_{P,C}$ close to $b_{\text{opt}}(P, \Omega_n)$ may in all cases still be obtained at the expense of a bad transient performance.

4.4 Damped Second Order System

Here we select a damped second order system

$$P(s) = k \, \frac{\omega_{\text{nat}}^2}{s^2 + 2\,\xi\,\omega_{\text{nat}}\,s + \omega_{\text{nat}}^2}$$

with $k = 10$, $\omega_{\text{nat}} = 5$.

In this section a critically damped ($\xi = 1$) second order, or equally two cascaded first order system, followed in the next subsection by a lightly damped ($\xi = 0.01$) second order system are considered.

The plant poles are located in

$$s = \omega_{\text{nat}}\,(-\xi \pm j\,\sqrt{1-\xi^2}).$$

The lightly damped system ($\xi = 0.01$) gives plant poles at $s \approx \pm j\,\omega_{\text{nat}}$; whereas for the critically damped system ($\xi = 1$) there are two poles at $s = -\omega_{\text{nat}}$.

4.4.1 Critically Damped

For this process $b_{\text{opt}}(P) \approx 0.55$, and therefore a great deal of flexibility in the design for obtaining both good robustness margins and transient

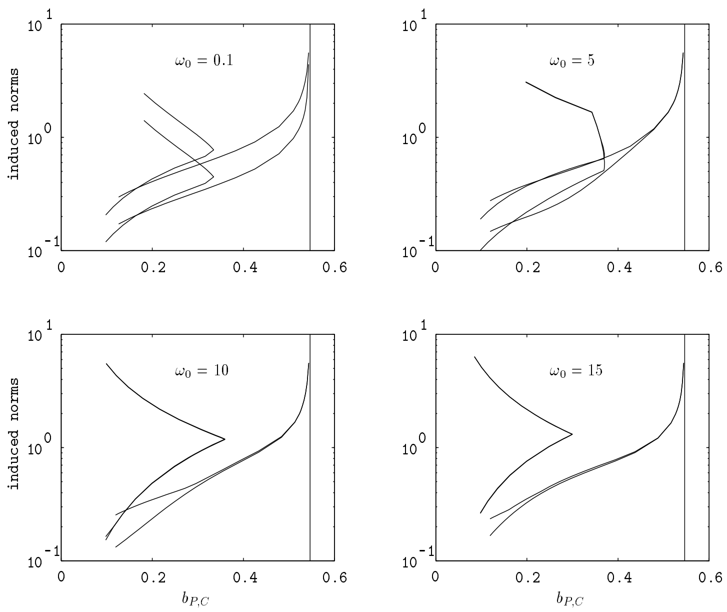

Figure 13: Loop shaping depicted as $\|P(I+CP)^{-1}\|_{\mathrm{tr}\leftarrow\mathcal{D}_3}$ and $\|P(I+CP)^{-1}\|_{\mathrm{step}}$ (2-norm) as a function of $b_{P,C}$ with $\beta \in [0.03, 8.5]$ and pole placement with $A_m = ((s+a)^2+\omega_0^2)\,(s+a)^4$ and $a \in [0.37, 6]$; $H(s) = s(s^2+\omega_0^2)$ for different ω_0.

performance is expected, as long as ω_0 is well within the bandwidth and therefore not limited by (14).

From Fig. 13 we see two things, as expected the loop shaping design ($W_\beta(s)$ again given by (2)) approaches the optimal $b_{P,C}$, and that the lower order pole placement controller with $A_m = ((s+a)^2+\omega_0^2)\,(s+a)^4$, gives worse transient performance but sufficient robustness. In the region where $b_{P,C} \in [0.25, 0.3]$ both design methods gives almost the same performance. The loop shaping controller, being of higher order, gives a slightly better transient performance for $\omega_0 = 1,\ 5$ rad/s. With $\omega_0 = 5$, a better robustness may be achieved as seen from the maximum $b_{P,C}$ obtained from this pole placement. Also from Fig. 13 (and later in Fig. 14 with $\omega_0 = 5$), in contrast to the former example, the system becomes less sensitive to the location of the closed loop poles.

Both for $\omega_0 = 10,\ 15$ rad/s, the open loop plant gain is high enough so that still $b_{\mathrm{opt}}(P, \Omega_3) = b_{\mathrm{opt}}(P)$. Figure 13 shows that the loop shaping design gives a smaller transient than the selected pole placement.

To analyse further the shapes of the different graphs depicting the trade-off between robustness and transient performance, the controller

$$
\begin{aligned}
C(s) &= \frac{c_4\, s^4 + c_3\, s^3 + c_2\, s^2 + c_1\, s + a^4(a^2+b^2)}{250\, s\,(s^2+\omega_0^2)\,(s-10+6a)} \qquad (23)\\
c_1 &= a^3(6a^2+4b^2) + \omega_0^2(250-150a) \ ; \ c_2 = 6a^2b^2 + \omega_0^2(75-60a) + 15a^4\\
c_3 &= a(4b^2+20a^2) - 6a\omega_0^2 + 250 - 150a \ ; \ c_4 = 75 + 15a^2 + b^2 - \omega_0^2 - 60a
\end{aligned}
$$

giving a pole placement of $A_m = ((s+a)^2+b^2)\,(s+a)^4$ is introduced. Note that the curves derived earlier in this section is for $b = \omega_0$.

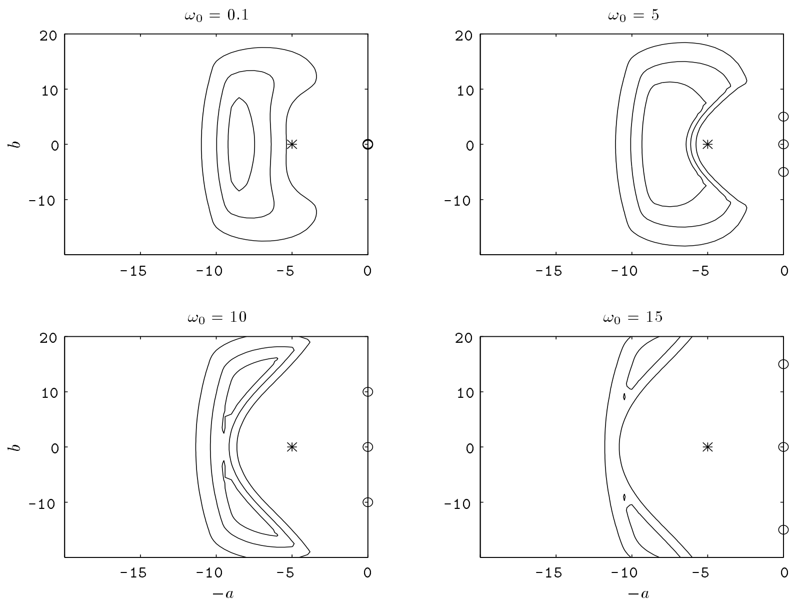

Figure 14: Robustness regions $b_{P,C} \geq \alpha$, $\alpha = \{0.2, 0.25, 0.3\}$, as a function of the closed loop poles, chosen according to $A_m = ((s+a)^2+b^2)\,(s+a)^4$, and $H(s) = s(s^2+\omega_0^2)$ with different internal model frequencies ω_0; open loop plant and controller poles is marked by '$*$' and '$\circ$' respectively.

By depicting $b_{P,C}$ as a function of the closed loop poles, we may gain more insight in how large $b_{P,C}$ we may expect for the selected structure for pole location (reducing the available degrees of freedom); and also how sensitive this solution is to parameter variations by looking at the size of the regions. From Fig. 14 and $\omega_0 = 0.1$ we note that a $b_{P,C}$ of at least 0.3 may be obtained, even by selecting all poles in one point, $a = 8.5$ and $b = 0$, giving $A_m = (s+8.5)^6$. For a higher internal model frequency $\omega_0 = \omega_{\text{nat}} = 5$ rad/s, Fig. 14 shows that the selection of closed loop poles may be done more freely. Again a $b_{P,C} > 0.3$ may be obtained by simply locating all poles in one point on the negative real axis, but better robustness is actually obtained by selecting two complex poles with a complex part of $\pm j\omega_0$.

For $\omega_0 = 0.1$ and $\omega_0 = 5$ rad/s, in Fig. 13, shows that both design methods give similar performance in the region of $b_{P,C} \in [0.25, 0.3]$, apart from

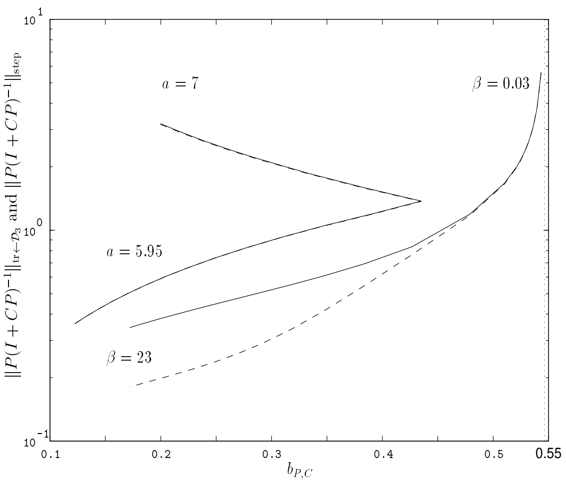

Figure 15: Loop shaping with $\beta \in [0.03, 23]$ and pole placement with $A_m = ((s+a)^2+\omega_0^2)\,(s+a)\,(s+c)^3$, $c = 4$ and $a \in [7, 25]$; $H(s) = s(s^2+\omega_0^2)$ and $\omega_0 = 5$.

the fact that the pole placement design never approaches the optimal robustness limit. Just to demonstrate how better robustness may be obtained by locating some of the poles closer to the open loop plant poles. There are two plant poles in $s = -5$ and the integrator pole in $s = 0$. For simplicity, the compromise of locating three of the closed loop poles in $s = -c$, where $c \in [0, 5]$ on the negative real axis. This is obtained by using the controller

$$
\begin{aligned}
C(s) &= \frac{c_4\,s^4 + c_3\,s^3 + c_2\,s^2 + c_1\,s + a^3c^3 + ab^2c^3}{s\,(s^2+\omega_0^2)\,(s+3\,(a+c)-10)} \qquad (24)\\
c_4 &= 3c^2 - \omega_0^2 + 75 + b^2 + 3a^2 - 30(a+c) + 9ac\\
c_3 &= c^3 + 3b^2c + 9ac^2 + a^3 - 3a\omega_0^2 - 3\omega_0^2c - 75c + ab^2 + 9a^2c - 75a + 250\\
c_2 &= -30\omega_0^2c + 3a^3c + 3ab^2c - 30a\omega_0 2 + 9a^2c^2 + 75\omega_0^2 + 3ac^3 + 3b^2c^2\\
c_1 &= 3a^3c^2 + 3a^2c^3 + 3b^2ac^2 - 75a\omega_0^2 - 75\omega_0^2c + 250\omega_0^2 + b^2c^3
\end{aligned}
$$

giving a pole placement of $A_m = ((s+a)^2+b^2)\,(s+a)\,(s+c)^3$. Note that with this selection of c the overall transient performance is reduced, giving rise to a higher transient power-energy induced norm. So, just as with the loop-shaping design, this is something we have to pay for increasing the robustness. Figure 15 shows compared with Fig. 13 that using this controller with $c = 4$, a $b_{P,C} \geq 0.4$ may be obtained. Using this simple trick we may, if necessary (in this case it is not), increase the robustness at the expense of poorer transient performance.

Finally, Fig. 16 shows that apart from the triple pole in $s = -c = -4$, the location of the remaining three poles are not that critical. Selecting a triple pole in $s = -a = -14$ $(b = 0)$ gives a $b_{P,C} > 0.3$ and good transient performance, taking into account that it is largely limited by the selection of c above. As the left boundary is curved, an off axis pole placement would in this case probably not give a large improvement on the transient performance.

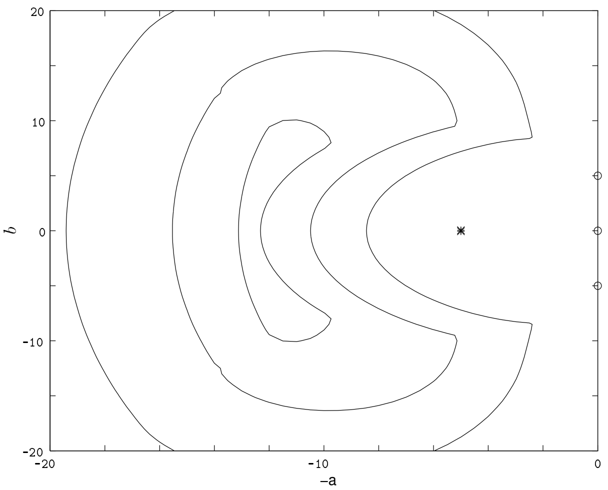

Figure 16: Robustness regions $b_{P,C} \geq \alpha$, $\alpha = \{0.2, 0.3, 0.4\}$, as a function of the closed loop poles, chosen according to $A_m = ((s+a)^2 + b^2)(s+a)(s+c)^3$ with $c = 4$ and internal model $H(s) = s(s^2 + 5^2)$; open loop plant and controller poles is marked by '$*$' and '$\circ$' respectively.

4.4.2 Lightly Damped

In this subsection we study a lightly damped system $\xi = 0.01$, to check whether there will be any additional constraints e.g. due to resonances. With $b_{\text{opt}}(P) \approx 0.41$, we note that this plant is harder to control than the former one.

Figure 17 shows that, apart from having overall poorer robustness and worse transient performance, nothing unexpected happens when the internal model mode cross the resonant mode. In fact, it is easier to place the closed loop poles when both the process and internal model modes are close together, and therefore, as shown in Fig. 17, the best pole placement design is obtained for $\omega_0 = 5$. For $\omega_0 \leq 5$, performance is also fairly close to the higher order loop shaping design. Overall speaking, the shapes of the 2-norm/$b_{P,C}$ graphs are similar to the ones in the last section, and the peak value for robustness will again decrease, for higher values of ω_0.

Next we again turn to depicting $b_{P,C}$ as a function of the closed loop

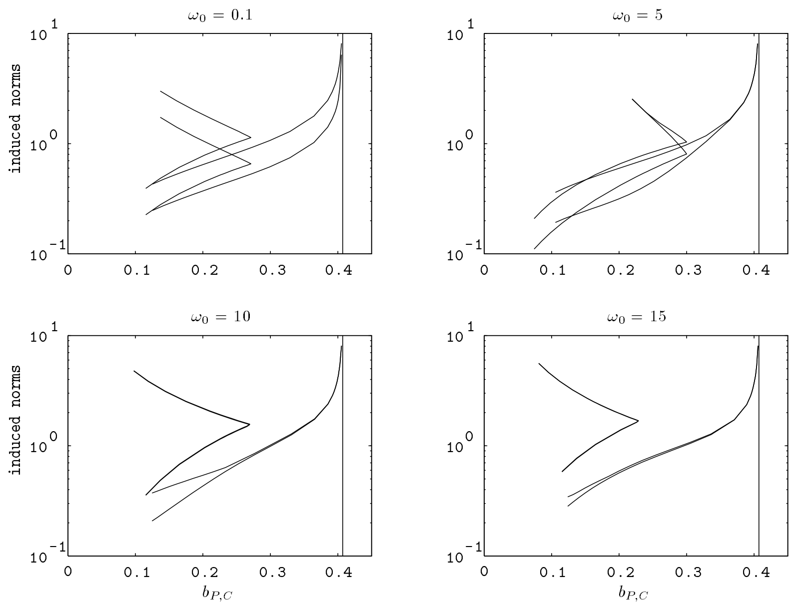

Figure 17: Loop shaping with $\beta \in [0.04, 28]$ and pole placement with $A_m = ((s+a)^2+\omega_0^2)\,((s+a)^2+\omega_{\text{nat}}^2)\,(s+a)^2$ and $a \in [5,15]$ with $H(s) = s(s^2+\omega_0^2)$ for different internal model frequencies ω_0.

poles. Using the controller

$$
\begin{aligned}
C(s) &= \frac{c_4\,s^4 + c_3\,s^3 + c_2\,s^2 + c_1\,s + a^6 + 25a^4 + a^4b^2 + 25a^2b^2}{250\,s\,(s^2+\omega_0^2)\,(s+6a-1/10)} \qquad (25)\\
c_1 &= 50ab^2 + 5/2\omega_0^2 + 100a^3 - 150a\omega_0^2 + 6a^5 + 4a^3b^2\\
c_2 &= 6a^2b^2 + 25b^2 - 24.99\omega_0^2 + 150a^2 + 15a^4 - 3/5a\omega_0^2\\
c_3 &= 4ab^2 + 5/2 + 20a^3 - 50a - 6a\omega_0^2 \;\; ; \;\; c_4 = b^2 - \omega_0^2 + 1/100 + 15a^2 - 3/5a
\end{aligned}
$$

gives a pole placement of $A_m = ((s+a)^2+b^2)\,((s+a)^2+\omega_{\text{nat}}^2)\,(s+a)^2$. With $\omega_0 = 0.1$, Fig. 18 confirms that a $b_{P,C}$ slightly higher than 0.25 may be obtained; and in this case better robustness had been obtained (against common rule of thumbs) by keeping all closed loop poles on the real axis, despite that the process has two off axis poles at $s = \pm\omega_{\text{nat}}$.

For a higher $\omega_0 = \omega_{\text{nat}} = 5$ rad/s, Fig. 18 shows that overall robustness is higher, and therefore to meet other design constraints, such as transient performance, is easier. In this case a $b_{P,C} > 0.3$ may again be obtained by locating all six poles around $s = -7$. For $\omega_0 = 10$, better robustness is obtained by locating the closed loop poles further away from the real axis than both the process and controller poles. So, in all cases presented in this section best robustness is obtained either further away or closer to the real axis, compared to rule of thumb kind of rules.

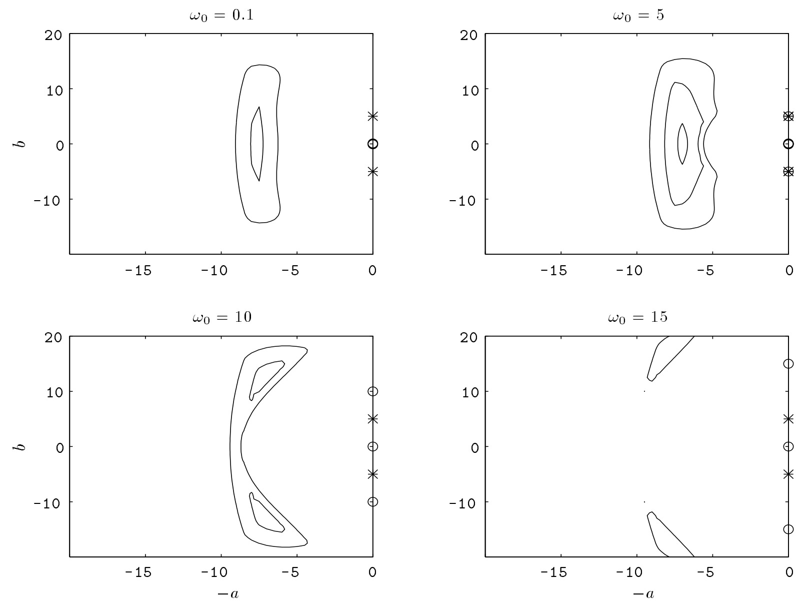

Figure 18: Robustness regions $b_{P,C} \geq \alpha$, $\alpha = \{0.2, 0.25, 0.3\}$, as a function of the closed loop poles, chosen according to $A_m = ((s+a)^2 + b^2)(s+a)^4$ with $H(s) = s(s^2 + \omega_0^2)$ for different internal model frequencies ω_0.

4.5 A CD Player Example

The final example consists of a Philips audio compact disc (CD) player CD930. CD930 consists of a two dimensional servo system, namely the radial loop and the focus loop. The cross interaction between the loops are negligible, and here only the radial loop is considered. The radial open loop plant is basically an undamped mass, modeled as a double integrator within the open loop bandwidth (neglecting the parasitic resonance dynamics at high frequency). When operating at an intermediate track where the rotation speed is 6 Hz, the open loop plant has a gain crossover frequency of around 400 Hz. We take the radial open loop plant to be

$$P(s) = \frac{(2\pi \cdot 400)^2}{s^2}.$$

At this track with the externally implemented Philips controller, the physical radial error contains a periodic signal of fundamental frequency 6 Hz [11].

The aim is to design a robust controller so as to cope with the variations over the full working range. In addition to a high bandwidth and a good robustness margin, the controller is designed to reject the d.c. as well as the 6 Hz ($\omega_0 = 12\pi$ rad/s) periodic disturbances arising from the rotation. We may therefore take the set of disturbances as $\Omega_3 \doteq \{0, \pm\omega_0\}$. The plant has a double pole at the origin and with the optimal robustness margin $b_{\text{opt}}(P) \approx 0.38$. The plant gain at 6 Hz is high enough so that $b_{\text{opt}}(P, \Omega_3) =$

$b_{\mathrm{opt}}(P)$. For the loop shaping design, the weighting function is again given by (2). On the other hand, the closed loop poles are selected to be $A_m = ((s+a)^2 + \omega_0^2)(s+a)^4$ for the poles placement design. As a result, the design parameters are $\beta \in [0.5, 15000]$ and $a \in [500, 4000]$ for the both design methods, respectively.

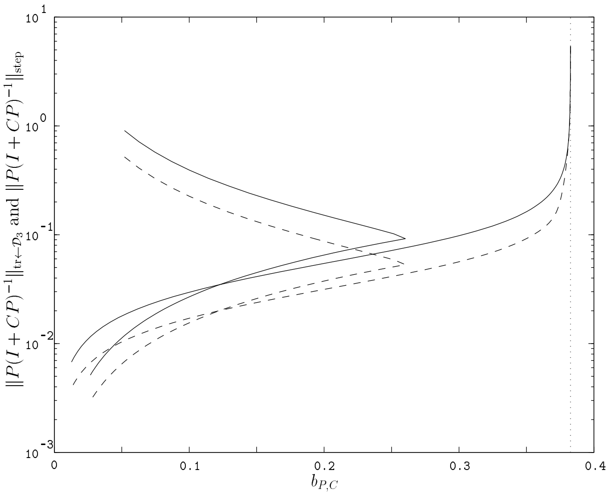

Figure 19: The transient power-energy induced norm as a function of $b_{P,C}$ for pole placement design, $A_m = ((s+a)^2 + \omega_0^2)(s+a)^4$, $a \in [500, 4000]$ and loop shaping with $\beta \in [0.5, 15000]$.

Figure 19 demonstrates the relation between two transient induced norms, namely $\|P(I+CP)^{-1}\|_{\mathrm{tr}\leftarrow\mathcal{D}_3}$ and $\|P(I+CP)^{-1}\|_{\mathrm{step}}$, and the gap metric robustness margin $b_{P,C}$. When β is small, the gap metric robustness margin is approaching the optimal value $b_{\mathrm{opt}}(P, \Omega_3)$ but the transient induced norms are blowing up, as seen in [10, 11]. When β is large, the induced norm is good but the gap metric robustness margin is poor. So, a practically interesting region is in the middle, where the both the gap metric robustness margin and the transient performance are satisfactory.

From Fig. 19 it is clear that, if it suffices with a robustness of $b_{P,C} = 0.25$, both design methods may be used. The lower order pole placement design, will give a slightly poorer transient performance. For pole placement design, the parameter $a = 1277$ gives

$$C_{PP}(s) = 3.872\frac{(s+362.1 \pm j720.2)(s+489.2 \pm j183.8)}{s(s^2+\omega_0^2)(s+7662)},$$

in which the power-energy induced-norm is 0.0873 (Fig. 19). On the other hand, for the loop shaping design with $\beta = 702$ the (model reduced) loop shaping controller is

$$C_{LS}(s) = 3.750\frac{(s+457.3 \pm j739.7)(s+455.9 \pm j140.2)}{s(s^2+\omega_0^2)(s+6998)},$$

and the transient power-energy induced norm is 0.0717 (Fig. 19). The open loop unweighted plant bandwidth is 400 Hz (i.e. 2513.3 rad/s) and the bandwidth for the closed loop $P(I + C_{LS}P)^{-1}$ is 543.0 Hz (i.e. 3411.5 rad/s), slightly above the open loop bandwidth.

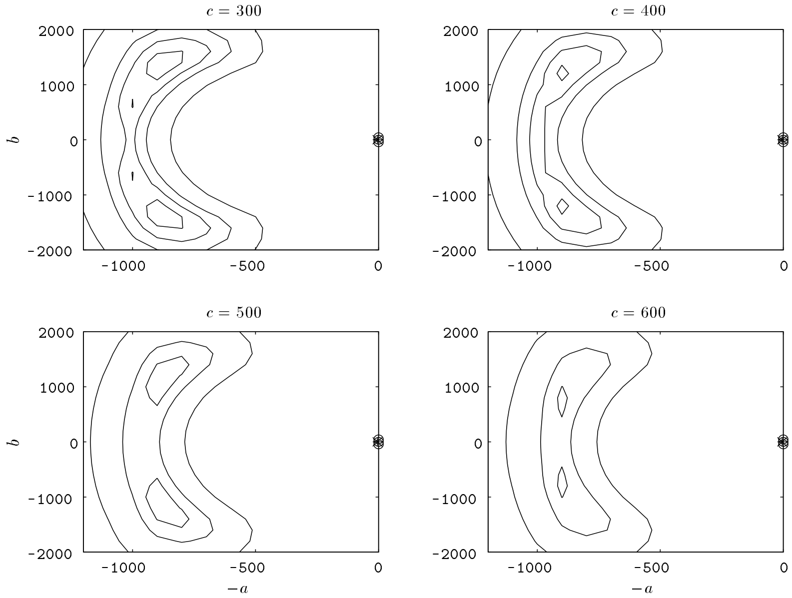

Figure 20: Robustness regions $b_{P,C} \geq \alpha$ for $\alpha \in \{0.2, 0.25, 0.275, 0.3\}$, as a function of pole placement for $A_m = ((s+a)^2+b^2)\,(s+a)\,(s+c)^3$, and $c = 300, 400, 500, 600$; open loop plant and controller poles is marked by '$*$' and '$\circ$' respectively.

From studying the closed loop poles obtained in the loop shaping design, we may conclude that the loop shaping controller roughly clusters all but three poles around $s \in [-400, -600]$ and place three poles further to the left; the same type of pole placement as studied earlier for the critically damped second order system. If we again introduce

$$\begin{aligned}
C(s) &= \frac{(c_4\, s^4 + c_3\, s^3 + c_2\, s^2 + c_1\, s + a^3c^3 + ab^2c^3)}{s\,(s^2+\omega_0^2)\,(s+3\,(a+c))} \qquad (26)\\
c_4 &= 9ac + 3c^2 + 3a^2 + b^2 - \omega_0^2\\
c_3 &= 9a^2c + ab^2 + a^3 + 9ac^2 - 3a\omega_0^2 - 3\omega_0^2c + c^3 + 3b^2c\\
c_2 &= 3b^2c^2 + 3a^3c + 3ab^2c + 9a^2c^2 + 3ac^3\\
c_1 &= 3a^3c^2 + 3ab^2c^2 + b^2c^3 + 3a^2c^3
\end{aligned}$$

giving $A_m = ((s+a)^2 + b^2)\,(s+a)\,(s+c)^3$, we get three poles nearer to the three open loop poles in the origin, and thereby a more robust solution. Again the transient response will largely be determined by c, the higher the c the higher the closed loop bandwidth and thereby the smaller the transient. For c = 300, 400, Fig. 20 shows that a $b_{P,C} > 0.3$ may be obtained. Improving the transient performance by increasing c results in worsening the robustness.

5 Conclusions

Robustness and transient performance of repetitive control systems were studied in the light of loop shaping and pole placement design. Both design methods clearly shows that faster response may be obtained at the expense of reduced robustness. A robustness close to the given bound $b_{\text{opt}}(P, \Omega_n)$ may in all cases above be obtained by loop shaping and letting $\beta \to 0$. In a case where this optimal robustness is low, it is suggested to use loop shaping. On the other hand, the loop shaping design is sensitive to the choice of the weighting function $W(s)$, and with the particular weighting function used here, better performance and robustness may in some cases be obtained by pole placement. Alternatively the chosen weighting function $W_\beta(s)$ may be cascaded by a stable and minimum phase biproper weighting function, which on the other hand gives rise to an even larger controller. So, in the end, for SISO LTI systems it is merely a matter of taste which design method being used. Graphs of robustness versus transient performance, on the other hand, gives clear indications on which of the designs to select, independent of the design method being used.

6 Acknowledgement

The first author is funded by *Norrbottens Forskningsråd* for the postdoctoral visit at Cambridge University Engineering Department, the academic year '96/'97. This support is greatly appreciated. The authors are grateful for the enlightening discussions with Dr. Malcolm C. Smith and his helpful suggestions.

References

[1] G.J. Balas, J.C. Doyle, K. Glover, A. Packard, and R. Smith. μ-analysis and synthesis toolbox user's guide: For use with matlab. Technical report, The MathWorks, Inc., 1994.

[2] B.A. Francis and W.M. Wonham. The internal model principle of control theory. *Automatica*, 12(5):457–465, 1976.

[3] T.T. Georgiou and M.C. Smith. Optimal robustness in the gap metric. *IEEE Trans. Autom. Contr.*, 35(6):673–686, 1990.

[4] G. Hillerström. On repetitive control. Doctoral Thesis 1994:155D, Luleå University of Technology, Sept. 1994.

[5] G. Hillerström and J. Sternby. Robustness properties of repetitive controllers. *Int. J. of Control*, 65(6):939–961, 1996.

[6] G. Hillerström and K.S. Walgama. Repetitive control theory and applications - a survey. In *Proceedings of the* 13^{th} *IFAC World Congress*, volume Vol. D, 1–6, San Francisco, July 1996.

[7] T. Kailath. *Linear Systems.* Prentice-Hall, 1980.

[8] G.F. Ledwich and A. Bolton. Repetitive and periodic controller design. *IEE Proc.-D*, 140(1):19–24, 1993.

[9] R.C.H. Lee. A compact disc player and repetitive control. First year report, University of Cambridge, May 1995.

[10] R.C.H. Lee and M.C. Smith. Some remarks on repetitive control systems. In *Proc. IEEE Conf. on Decision and Control*, 2023–2024, Kobe, Japan, 1996.

[11] R.C.H. Lee and M.C. Smith. Robustness and trade-offs in repetitive control. *Submitted*, 1997.

[12] C.-A. Lin and S.-J. Ho. Controller design for linear multivariable systems with periodic inputs. *IEE Proc.-D*, 139(1), 1992.

[13] D.C. McFarlane and K. Glover. Robust controller design using normalized coprime factor plant descriptions. *Lecture Notes in Control and Information Sciences*, 138, 1990.

[14] R.H. Middleton, G.C. Goodwin, and R.W. Longman. A method for improving the dynamic accuracy of a robot performing a repetitive task. *Int. J. Robotics Research*, 8(5):67–74, 1989.

[15] S. Rönnbäck and J. Sternby. A design algorithm for anti–windup compensators – polynomial approach. In *Proc IFAC World Congress*, volume VIII, 509–514, 1993.

[16] M. Tomizuka, T.-C. Tsao, and K.-K. Chew. Discrete-time domain analysis and synthesis of repetitive controllers. In *Proc. of the Am. Control Conference*, 860–866, 1988.

[17] G. Vinnicombe. Measuring the robustness of feedback systems. Doctoral thesis, University of Cambridge, 1993.

[18] K. Zhou, Doyle J., and Glover K. *Robust and Optimal Control.* Prentice Hall, 1995.

A Code

This section shows examples of the codes being used for computations in this report. For clarity, the Maple prompt of `>` and Matlab prompt of `>>` is added to the beginning of each line. The code is split up into the different parts and commented in more detail.

A.1 Initialization, 2-norm and Robustness

Initialization We begin with defining the plant, internal model frequency ω_0 (and for improved speed also the $\mathtt{w2} = \omega_0^2$) and the tolerance in the $b_{P,C}$ calculation.

```
>> tol=1e-8;                        % Tolerance for the Bpc calculation
>> sys=nd2sys([sqrt(2)],[1,1]);  % Process model
>> w=1; w2=w^2;                     % Internal model frequency of 1 rad/s
>> [asys,bsys,csys,dsys]=unpck(sys);
```

2-norm calculation This code implements the power-energy induced norm, based on the observability grammian matrix as presented in Section 2.

```
>> [asys1,bsys1,csys1,dsys1]=unpck(sysk);
>> [ac,bc,cc,dc]=feedback(asys,bsys,csys,dsys,asys1,bsys1,csys1,dsys1,1);
>> closedloop=pck(ac,bc,cc,dc);
>> [closedbal,sig]=sysbal(closedloop,1e-8); % Create balansed realization
>> [acbal,bcbal,ccbal,dcbal]=unpck(closedbal);
>> grammian=gram(acbal,bcbal);  % grammian of closed loop
>> grammianroot=chol(grammian);
>> mat=[grammianroot*inv(-acbal)*bcbal];
>> nstep(i)=sqrt(mat'*mat); % Calculate 2-norm of the step response
>> mat=[grammianroot*inv(-sqrt(-1)*w*eye(size(acbal))-acbal)*bcbal \
>>      mat grammianroot*inv(sqrt(-1)*w*eye(size(acbal))-acbal)*bcbal];
>>  n(i)=sqrt(max(real(eig(mat'*mat)))); % Power-energy induced norm
```

where `sysk` is the loop shaping controller `sysok` or the pole placement controller `sysk1` below.

Robustness, $b_{P,C}$ There are already functions in the μ-tools toolbox for Matlab for calculating the $b_{P,C} = \mathtt{rmar}$ and $b_{\mathrm{opt}}(P) = \mathtt{emax}$.

```
>> [rmar,erow]=xmargin(sys,sysk,tol); % The Robustness margin in rmar
>> [syskopt,emax,sysobs]=ncfsyn(sys,1); % 1 => optimally robust controller
```

The function `xmargin` is the updated version of `emargin`.

A.2 Loop Shaping

A Matlab code for calculating the loop shaping controller with weighting function given by (2), would be (`be(i)` is a vector containing the β values, and $\omega_0^2 =$ `w2`)

```
>> % the weighting function (with poles at 0, =/- j w)
>> internal=nd2sys(conv([1 be(i)],[1 2*be(i) be(i)^2+w2]),\
>> conv([1 0],[1 0 w2]));
>> sysw=mmult(sys,internal);   % the weighted plant
>> % sysoktemp = unweighted controller
>> [sysoktemp,loopshapeemax]=ncfsyn(sysw,1);
>> sysok=mmult(sysoktemp,internal);  % the final weighted controller
>> % the actual robustness margin for P, WC
>> [rmar,erow]=xmargin(sys,sysok,tol);
```

gives the loop shaping controller as `sysok` with robustness margin $b_{P,C} =$ `rmar`.

A.3 Pole Placement

As the general Maple code is based on lists for polynomial coefficients, it tends to look a bit messy; e.g.

```
> Cs:=[seq(s[i],i=0..degree(A,s)+degree(H,s)-1)];
> Cr:=subs(r[0]=1,[seq(r[i],i=0..degree(A,s)-1)]):
> S:=convert({seq(Cs[i+1]*s^i,i=0..degree(A,s)+degree(H,s)-1)},'+');
> R:=convert({seq(Cs[i+1]*s^i,i=0..degree(A,s)-1)},'+');
```

instead of

```
> S:=s0+s1*s+s2*s^2+s3*s^3+s4*s^4;
> R:=1;
```

for a first order process, with $H(s) = s\,(s^2 + \omega^2)$. Therefore, here, only one of the previous examples

```
> A:=s+1: B:=sqrt(2):  # The process
> H:=s*(s^2+w^2):      # Disturbance model
> #    Minimal order controller
> S:=s0+s1*s+s2*s^2+s3*s^3:   # deg(A)+deg(H)-1
> R:=1:                       # deg(A)-1
> Am:=collect(expand(A*H*R+B*S),s):  # Closed loop polynomial
> # Select CL polynomial of deg 2*deg(A)+deg(H)-1, e.g.
> Amd:=expand(((s+a)^2+b^2)*(s+a)^2):
> solve(map(x->x=0,{coeffs(collect(Amd-Am,s),s)}),{s0,s1,s2,s3});
```

for which Maple replies

$$\{s1 = \frac{1}{2}(2b^2a - w^2 + 4a^3)\sqrt{2}, s2 = \frac{1}{2}(b^2 - w^2 + 6a^2)\sqrt{2}, s0 = \frac{1}{2}a^2(a^2 + b^2)\sqrt{2},$$
$$s3 = \frac{1}{2}(-1 + 4a)\sqrt{2}\}$$

is given.

A.4 Graphs

In this section example codes for producing the robustness vs transient performance graphs, and $b_{P,C}$ as a function of pole placement graphs are shown. The parts with %% refers to the previous parts in this Appendix.

A.4.1 Robustness vs Transient Performance

```
>> al=[0.37:0.02:0.68,0.7:0.15:6]'; %   scan in the pole a.
>> m=length(al); >> be=logspace(-1,1,m); >>
>> %% Initialize
>>
>> em=zeros(l); emloop=zeros(l);
>> n=zeros(l); nloop=zeros(l);
>> nstep=zeros(l); nsteploop=zeros(l);
>>
>> for i=1:m,
>>  % Pole-placement controller
>>  a=al(i);
>>  s3=4*a-1; s2=6*a^2-w2; s1=-w2+4*a^3; s0=a^4;  % for Am = (s+a)^4
>>  sysk1=nd2sys(-[s3/b,s2/b,s1/b,s0/b],[1,0,w2,0]);
>>  em(i,j)=xmargin(sys,sysk1,tol);
>>
>>  %% Calculate 2-norm according to previous section
...
>>  n(i)=sqrt(max(real(eig(mat'*mat))));
>>
>>  %% Loopshaping controller
>>  internal=nd2sys(conv([1 be(i)],[1 2*be(i) be(i)^2+w2]),\
>>     conv([1 0],[1 0 w2]));
...
>>  [rmar,erow]=xmargin(sys,sysok,tol);
>>
>>  emloop(i)=rmar;   % the actual robustness margin for P, WC
>>
>>  %% Calculate 2-norm
...
```

```
>>  nloop(i)=sqrt(max(real(eig(mat'*mat))));
>> end  % for
>> % Maximum robustness for pole placement
>> [ax,bx]=max(em); fprintf('bpc= %g, 2-norm= %g, a=%g \n',ax,n(bx),al(bx));
>> ymin=10^floor(log10(min([n' nloop' nstep' nsteploop'])));
>> ymax=10^ceil(log10(max([n' nloop' nstep' nsteploop'])));
>> semilogy(em,n,emloop,nloop,em,nstep,emloop,nsteploop,[bpclim \
>>    bpclim],[ymin ymax]);
>> xlabel('bPC'); ylabel('2-norm');
```

A.4.2 Robustness Regions

Maps of obtainable $b_{P,C}$ as a function of pole placement were obtained variants of the following Matlab code.

```
>> bpc=zeros(40,81);
>> for i=1:40,
>>   for j=0:40,
>>    a=i/10; b=j/5; % Scale mesh to appropriate range (i,j) -> (a,b)
>> % Pole placement obtained from the Maple session
>> sysk1=nd2sys(-[(4*a-1)/sqrt(2),(b^2-w2+6*a^2)/sqrt(2),\
>> (4*a^3+2*a*b^2-w2)/sqrt(2), a^2*(a^2+b^2)/sqrt(2)],[1,0,w2,0]);
>>      bpc(i,41+j)=xmargin(sys,sysk1,tol);  % Store in the mesh, and
>>      bpc(i,41-j)=bpc(i,41+j);             % mirror in the real axis
>>   end;
>> end;
>>
>> contour([-0.1:-0.1:-4],[-8:0.2:8],bpc',[0.2,0.3,0.4,0.5]);
>> axis([-4 0 -8 8]); hold, plot(-1,0,'*',[0 0],[w -w],'o'); hold
>> xlabel('a'); ylabel('b');
```